APPENDIX

CONTROLLING THE INTERFACES OF SUPRAMOLECULAR HYDROGELS FOR TISSUE CULTURE APPLICATION

EFSTRATIOS D. SITSANIDIS

July 2018

LIST OF FIGURES

Chapter 2

SUPPLEMENTARY INFORMATION

In this section all the spectroscopic data reported in chapter 2 is provided. Two-dimensional NMR spectra (HSQC, HMBC, COSY and NOESY) are not shown herein as were used only for assisting interpretation of ^{1}H and ^{13}C NMR spectra.

Solution spectra reported in chapter 4 of hydrogelators GalNHFmoc **62**, GlcNHFmoc **63** and Fmoc-F-F **68** in methanol are given to facilitate interpretation of the SRCD studies.

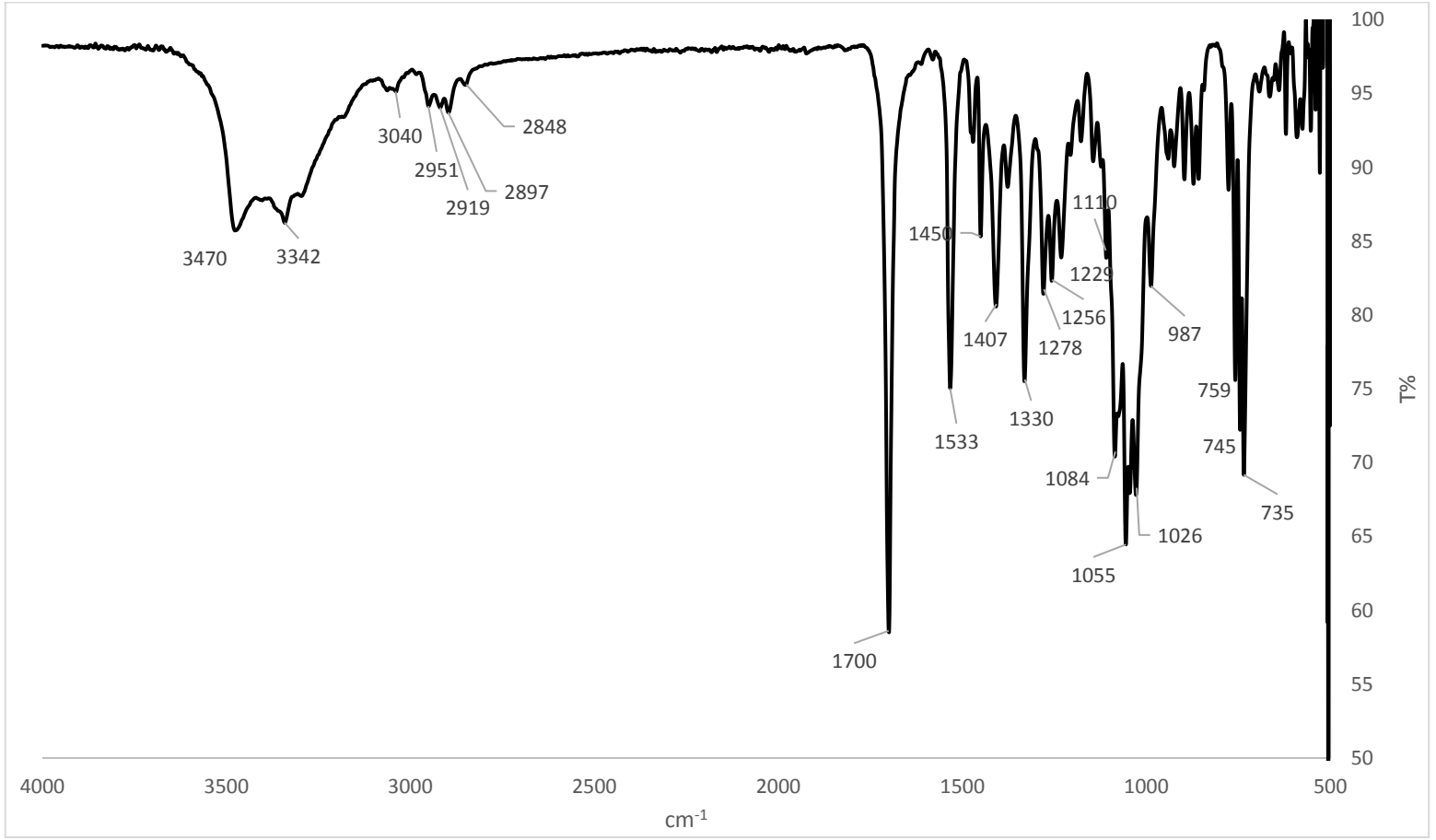

Figure A 2.1 IR (neat) of *N*-Fmoc-D-galactopyranosylamine **64**

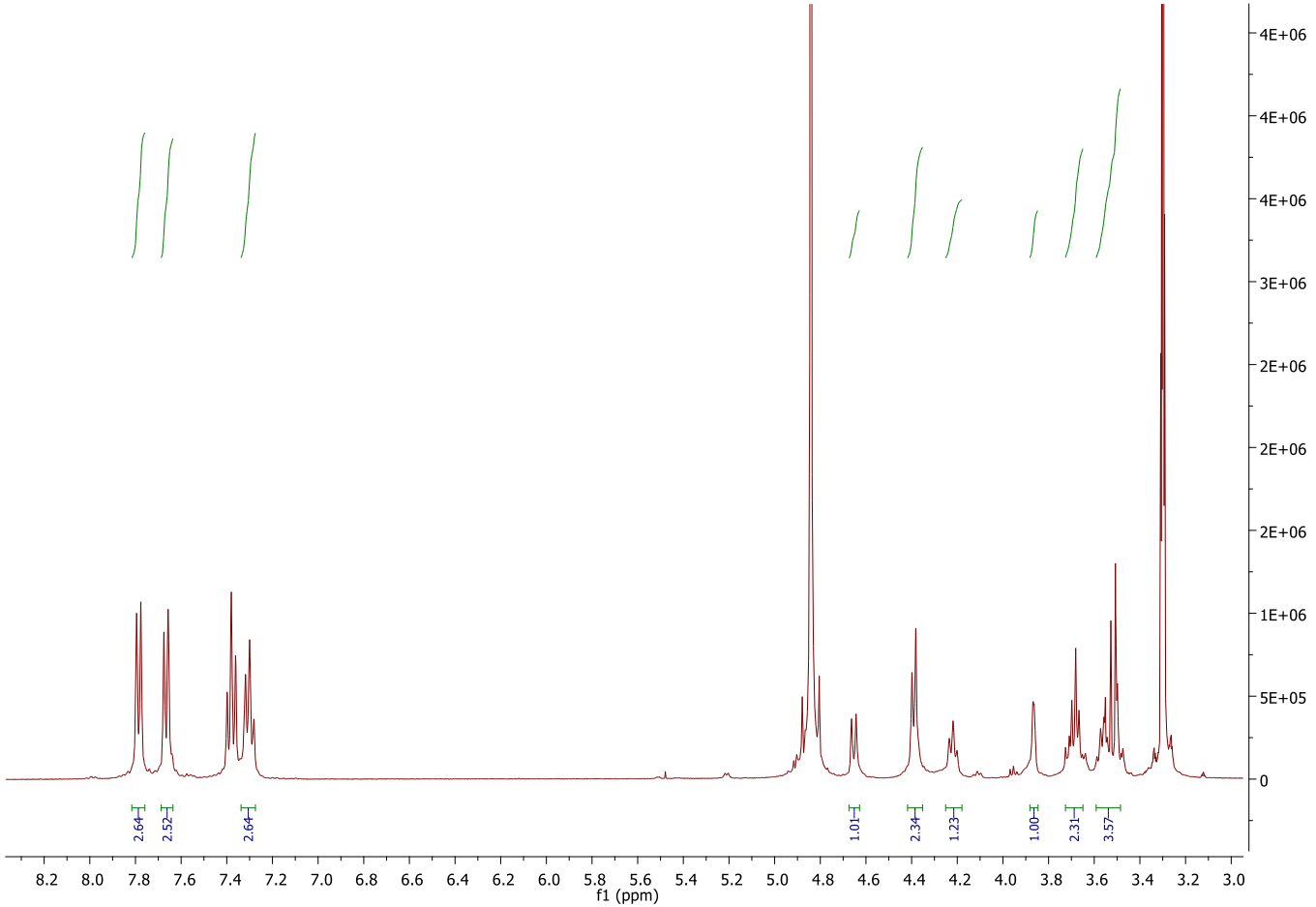

Figure A 2.2 ^{1}H NMR (500 MHz, methanol-d_3) of *N*-Fmoc-D-galactopyranosylamine **64**

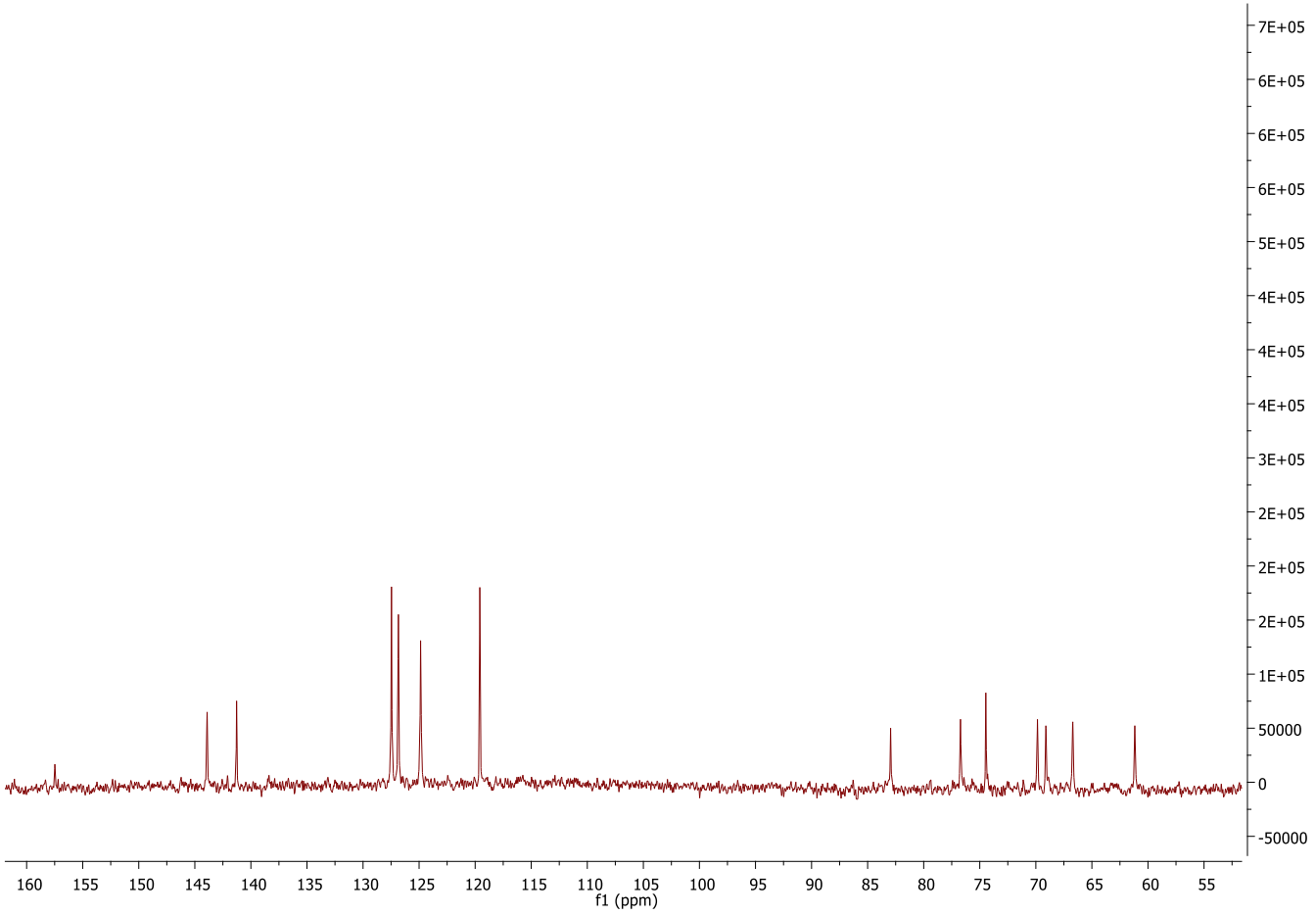

Figure A 2.3 ^{13}C NMR (101 MHz, methanol-d_3) of *N*-Fmoc-D-galactopyranosylamine **64**

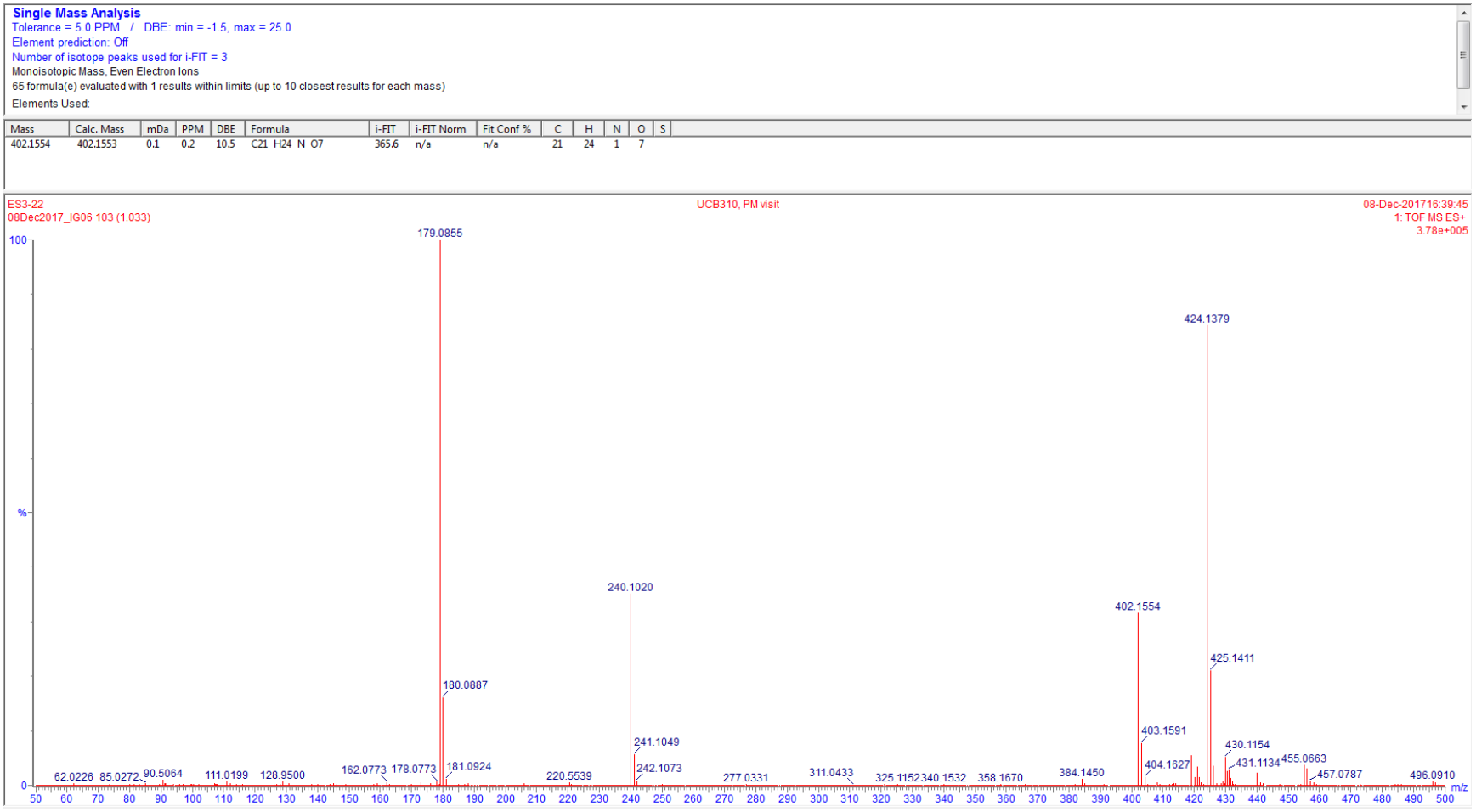

Figure A 2.4 HR-MS of *N*-Fmoc-D-galactopyranosylamine **64**

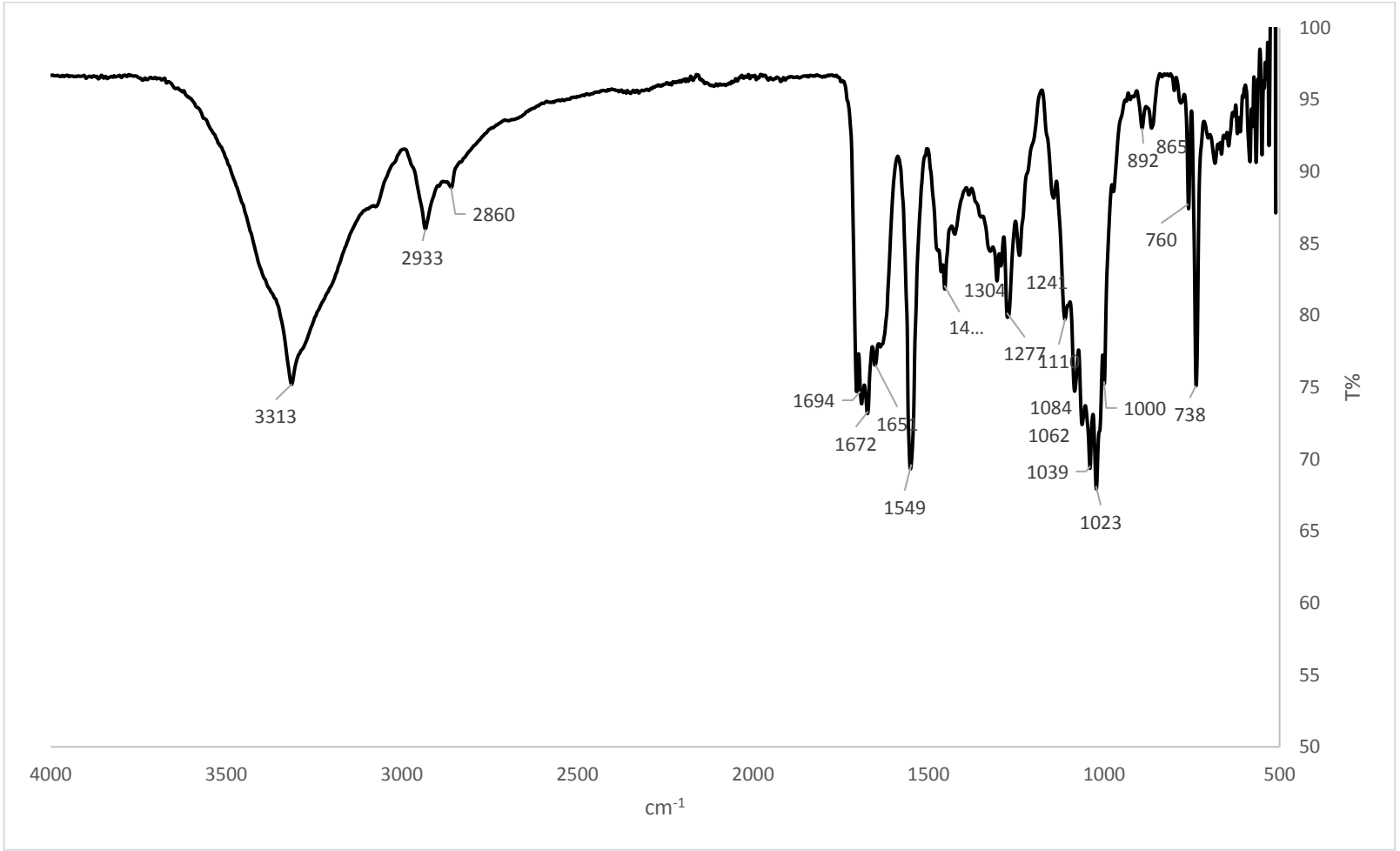

Figure A 2.5 IR (neat) of *N*-Fmoc-D-glucopyranosylamine **65**

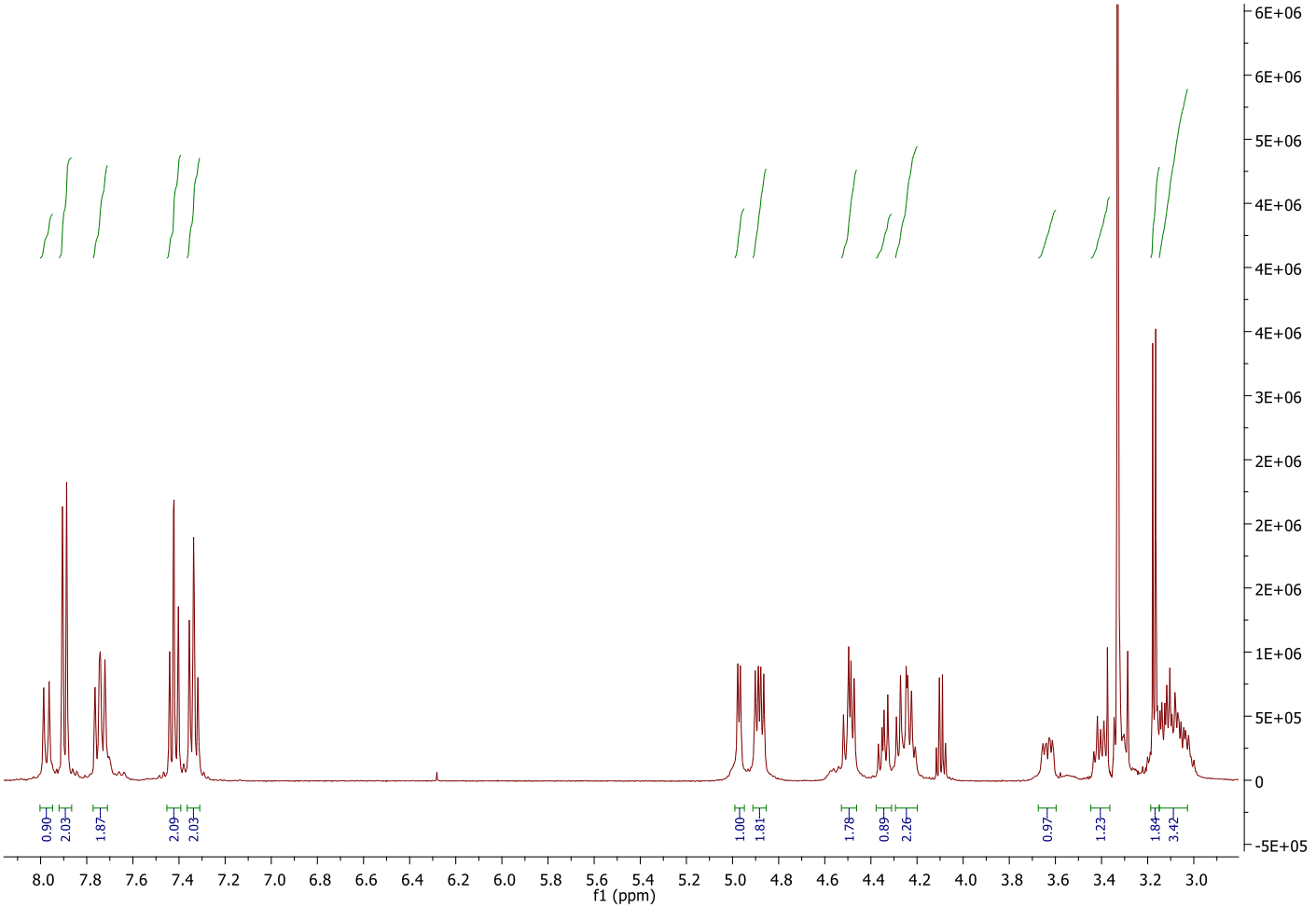

Figure A 2.6 ^{1}H NMR (500 MHz, dmso-d_6) of *N*-Fmoc-D-glucopyranosylamine **65**

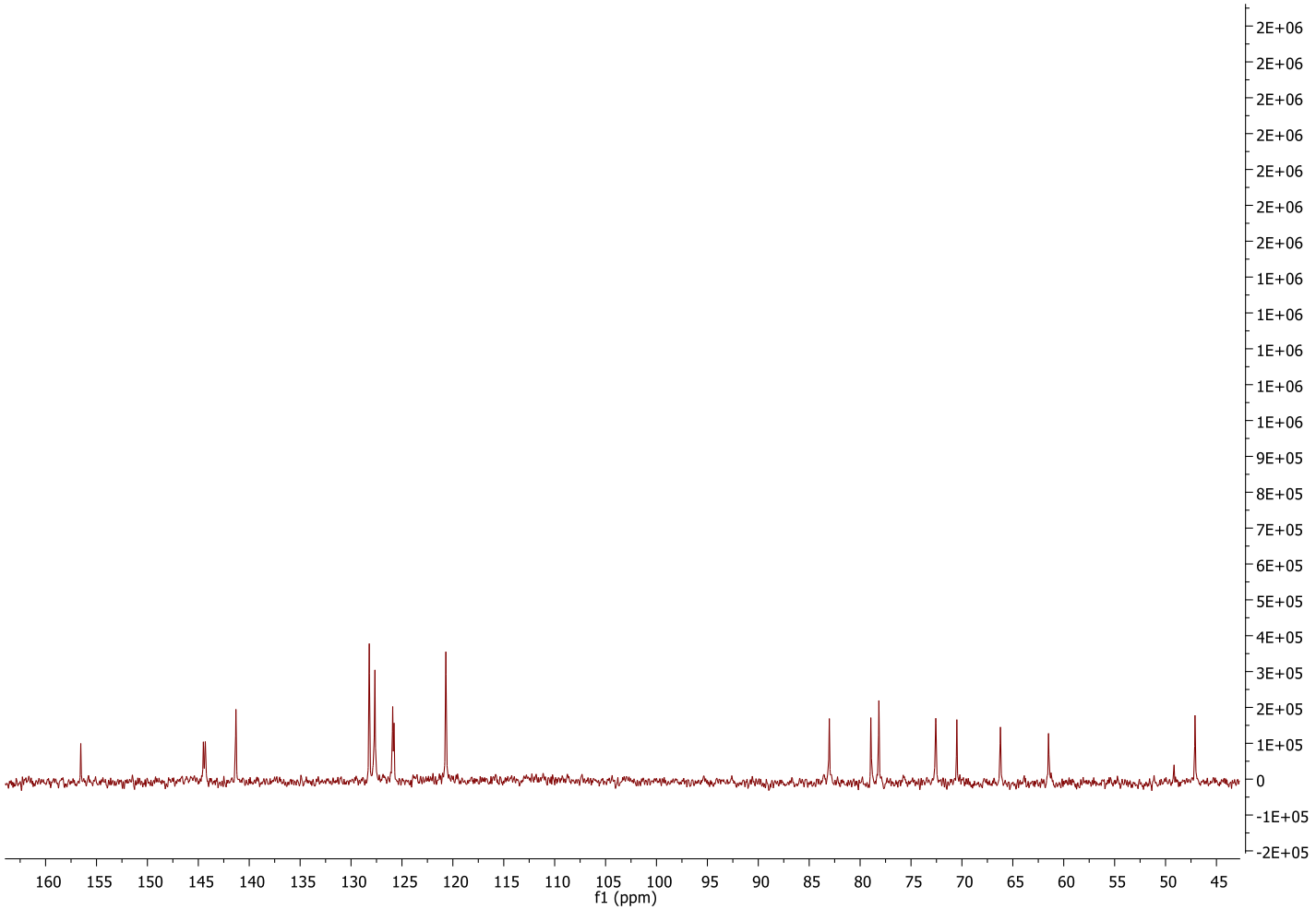

Figure A 2.7 ^{13}C NMR (126 MHz, dmso-d_6) of *N*-Fmoc-D-glucopyranosylamine **65**

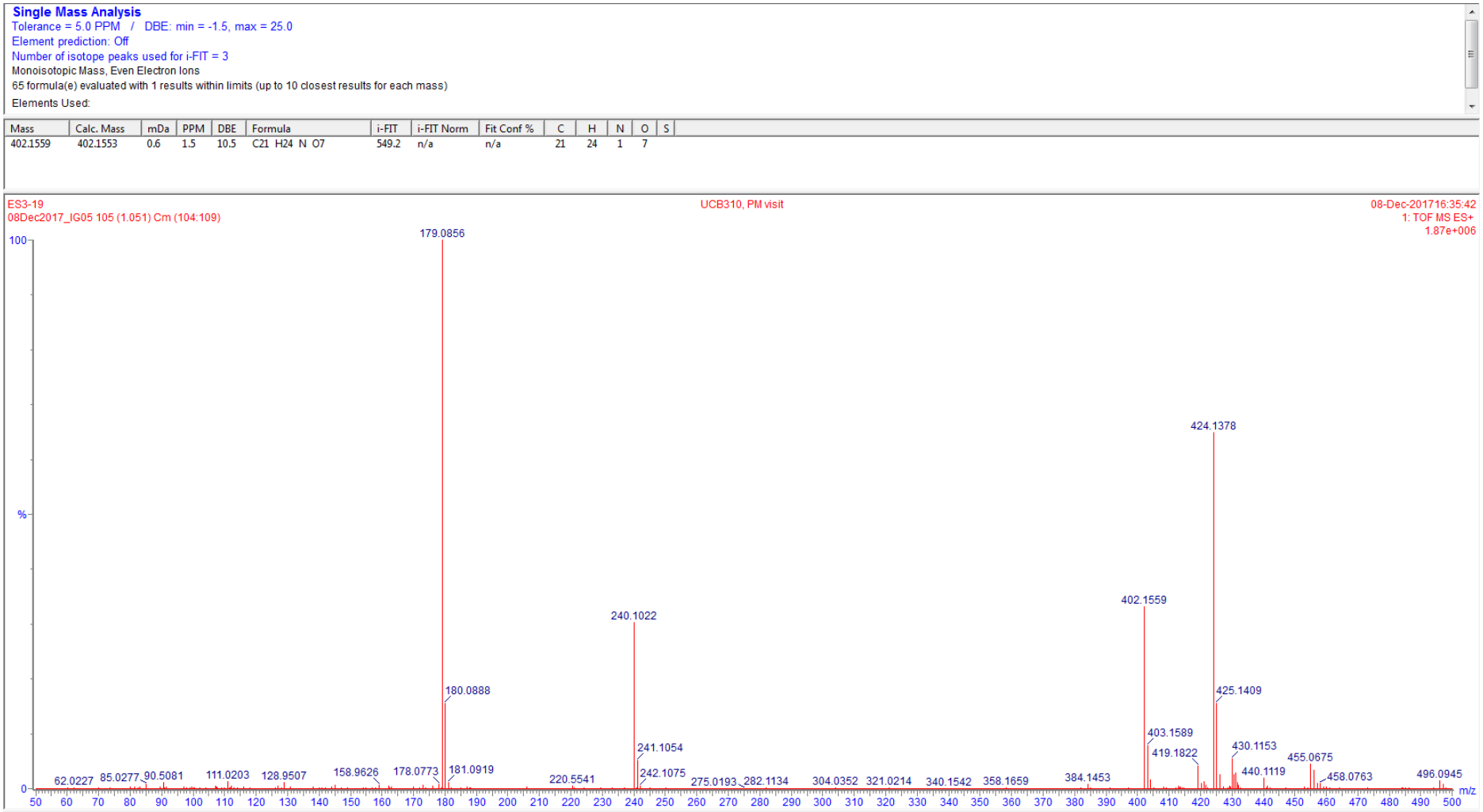

Figure A 2.8 HR-MS of *N*-Fmoc-D-glucopyranosylamine **65**

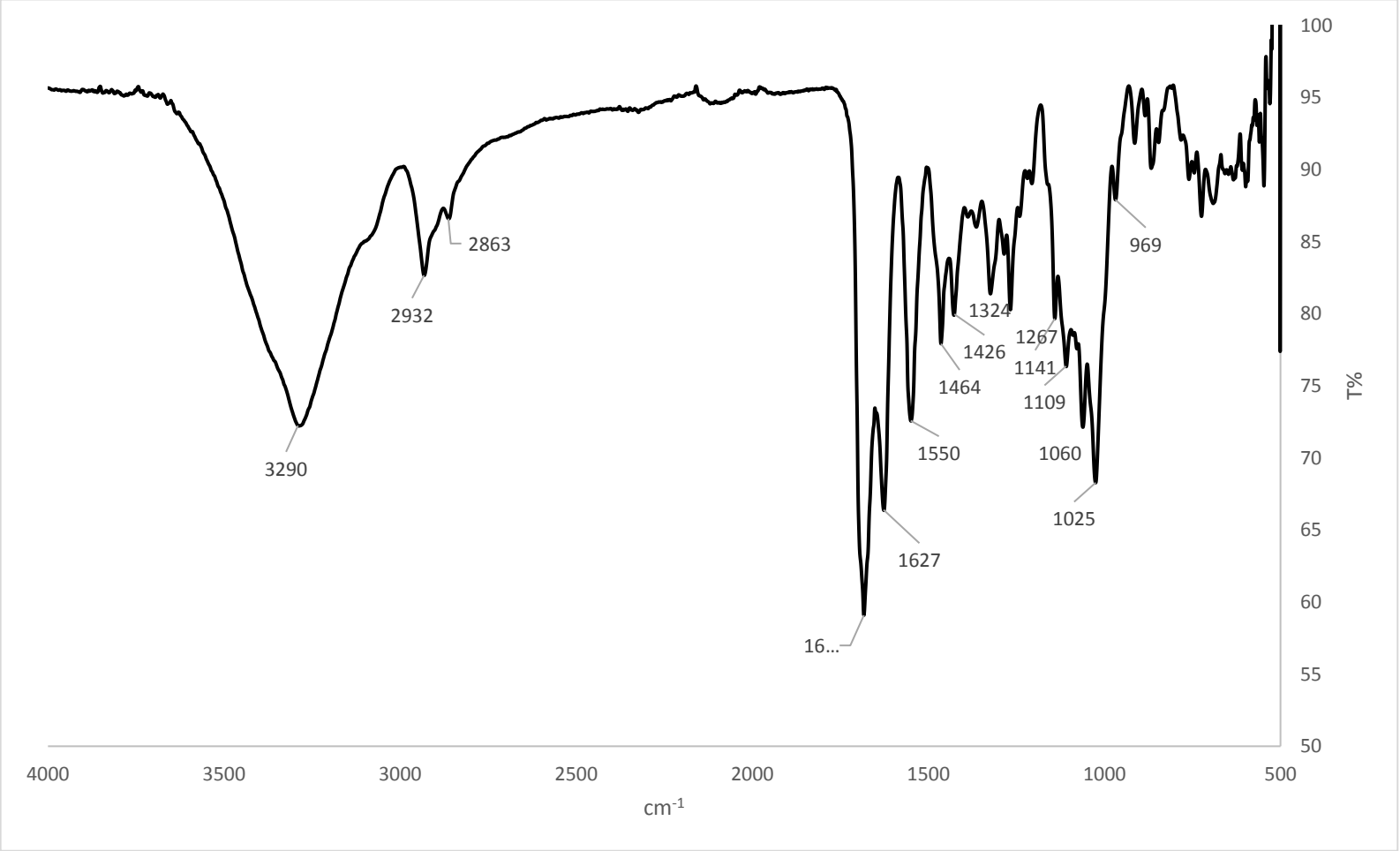

Figure A 2.9 IR (neat) of Biotin-D-glucosamine **67**

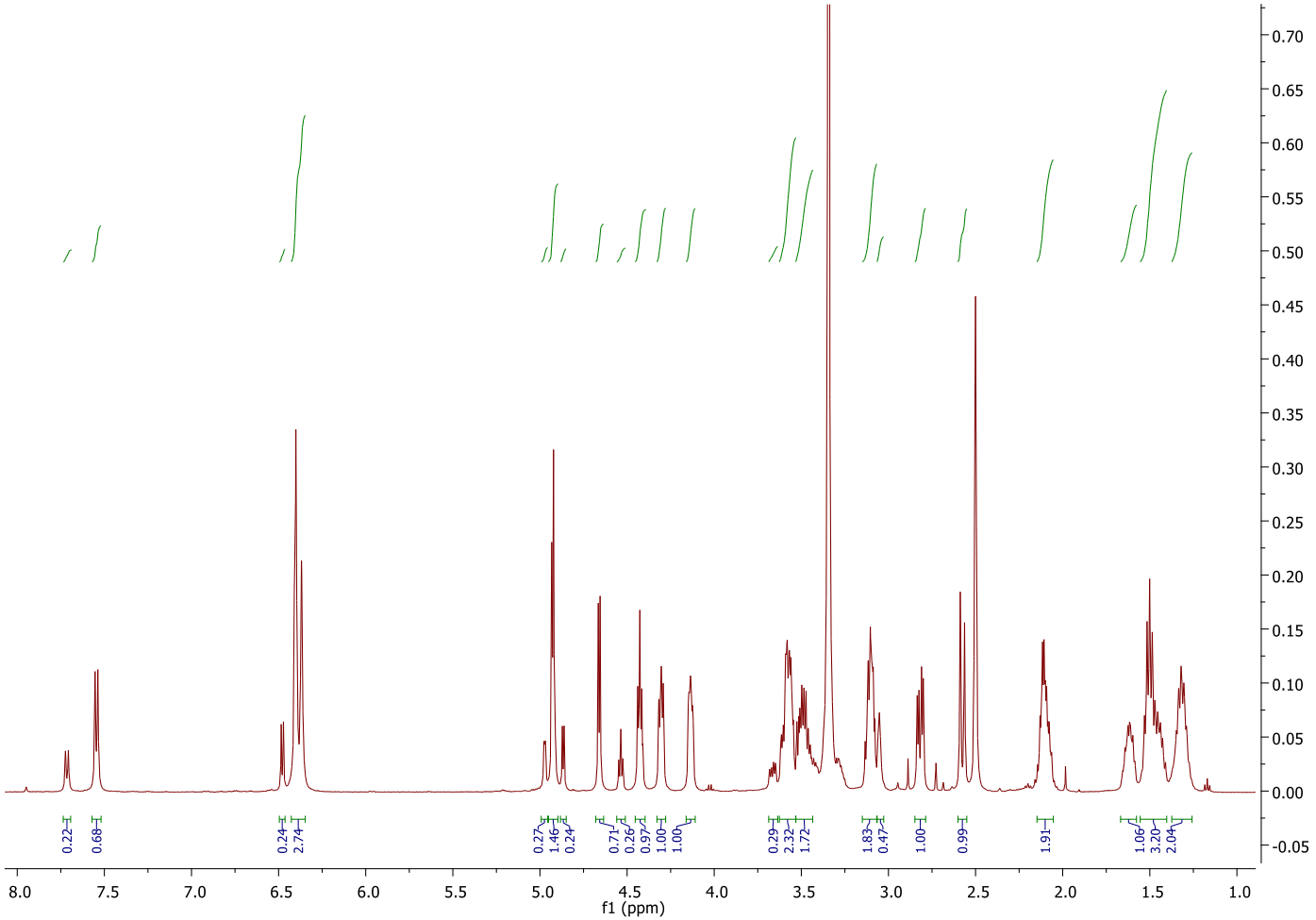

Figure A 2.10 ^{1}H NMR (500 MHz, dmso-d_6) of Biotin-D-glucosamine **67**

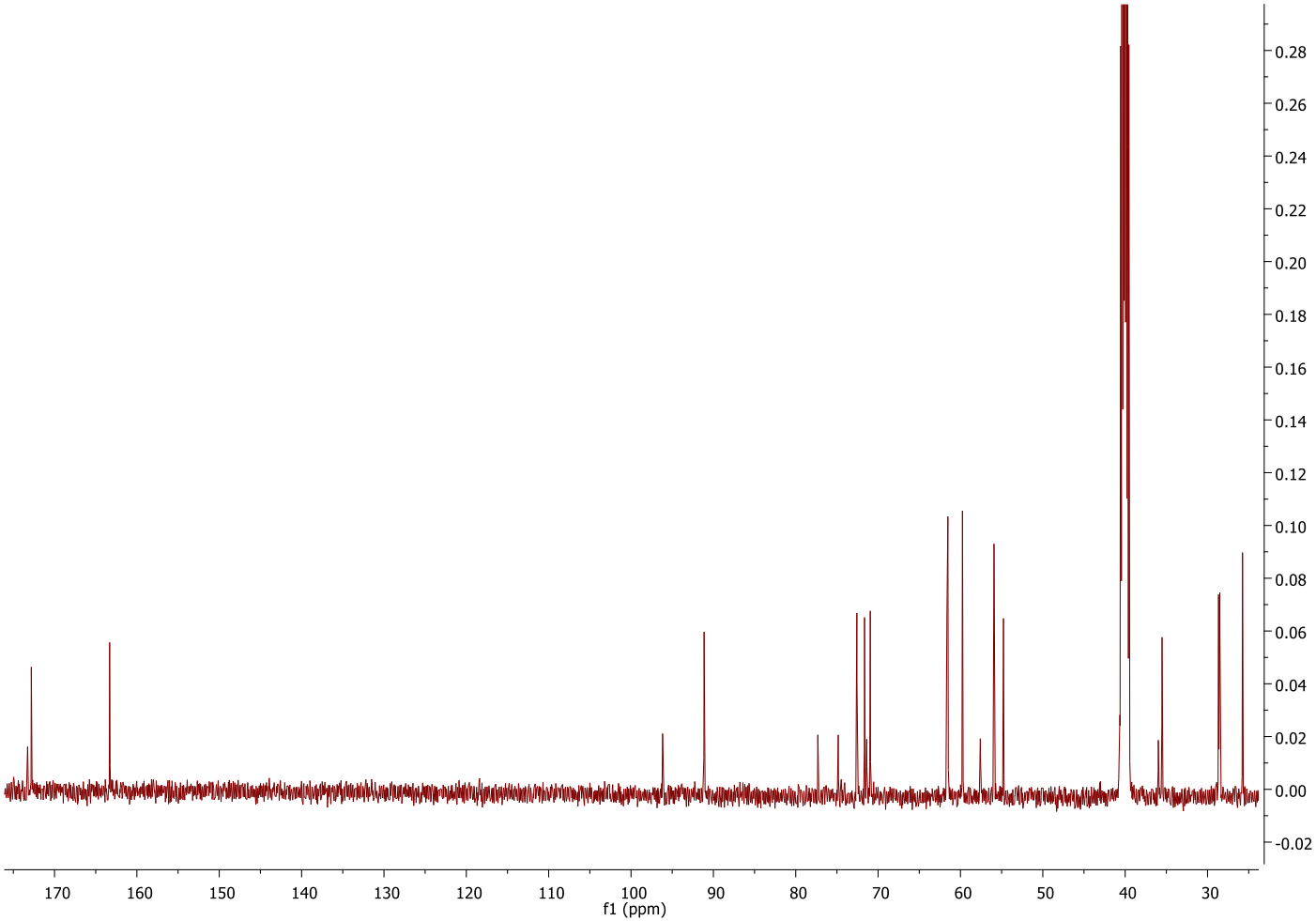

Figure A 2.11 ^{13}C NMR (126 MHz, dmso-d_6) of Biotin-D-glucosamine **67**

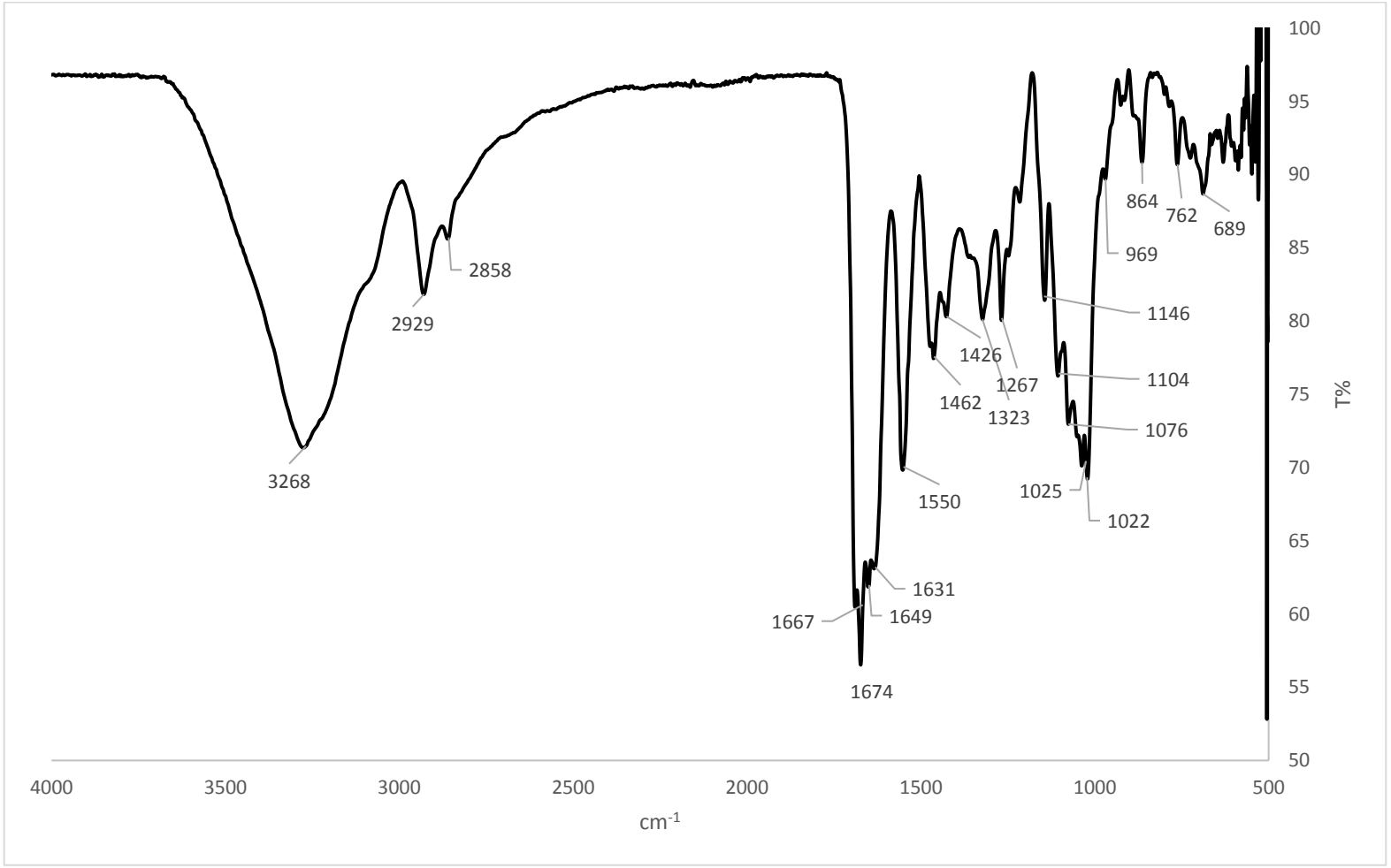

Figure A 2.12 IR (neat) of Biotin-D-galactosamine **66**

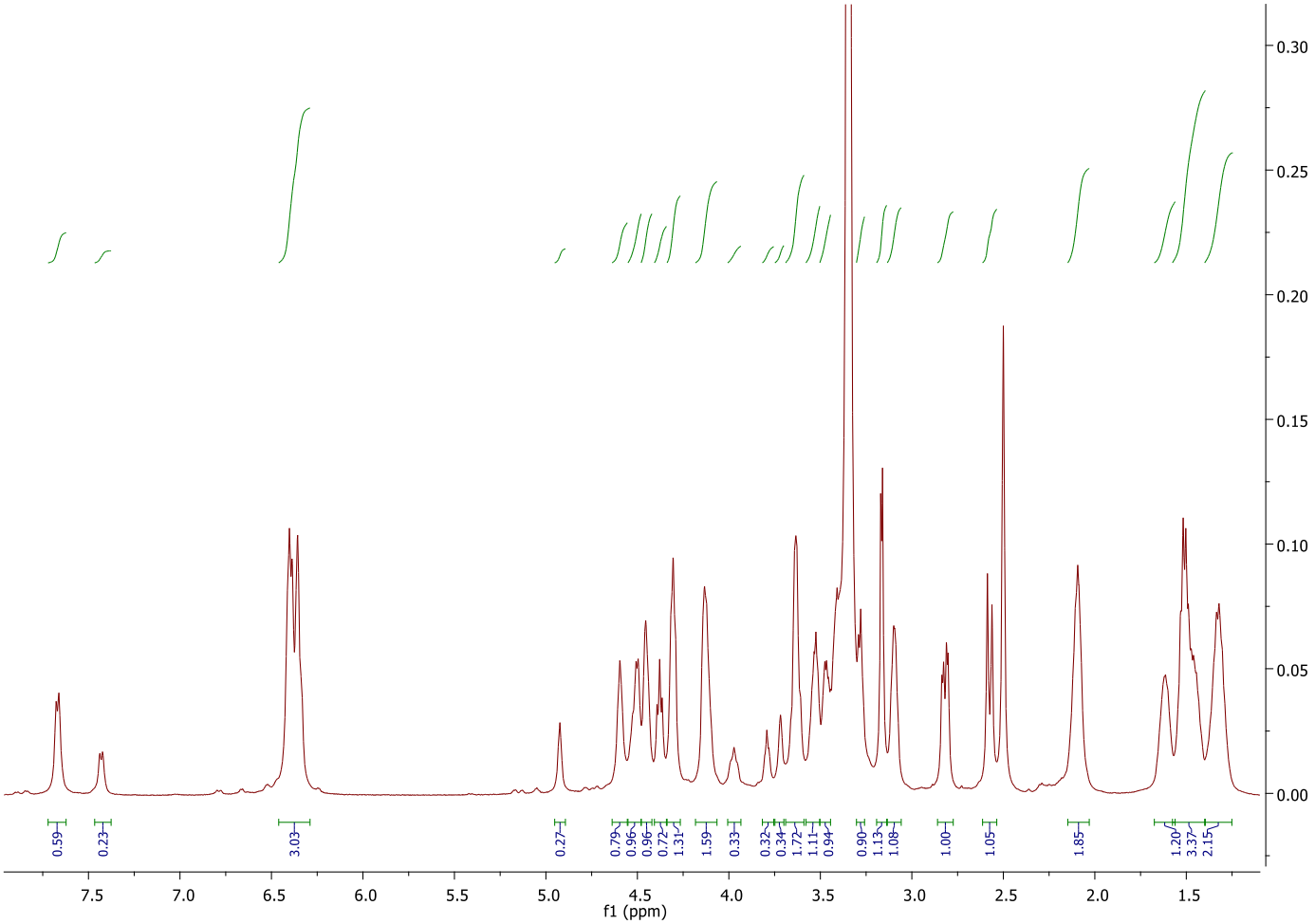

Figure A 2.13 ^{1}H NMR (500 MHz, dmso-d_6) of Biotin-D-galactosamine **66**

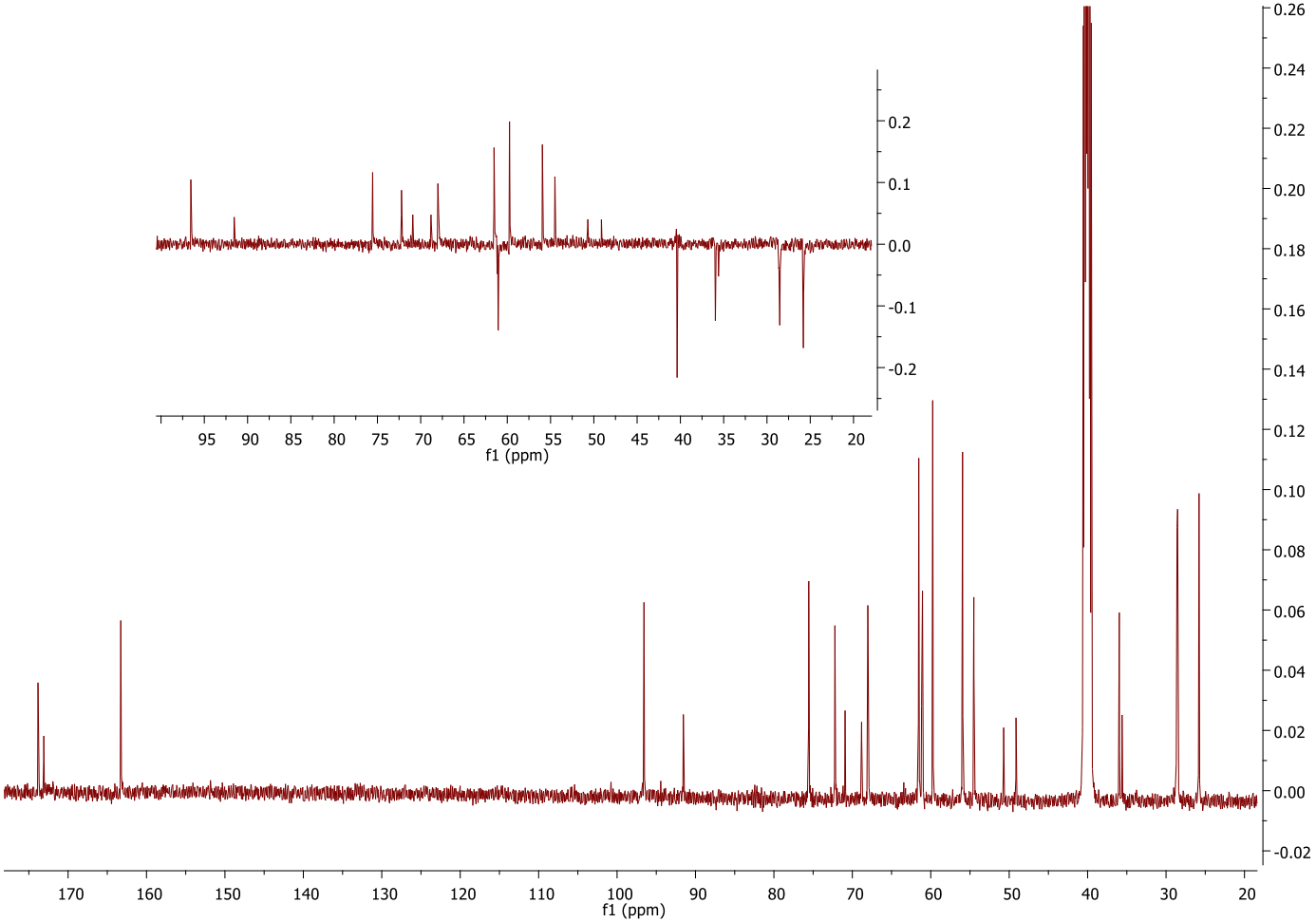

Figure A 2.14 ^{13}C NMR (126 MHz, dmso-d_6) of Biotin-D-galactosamine **66**

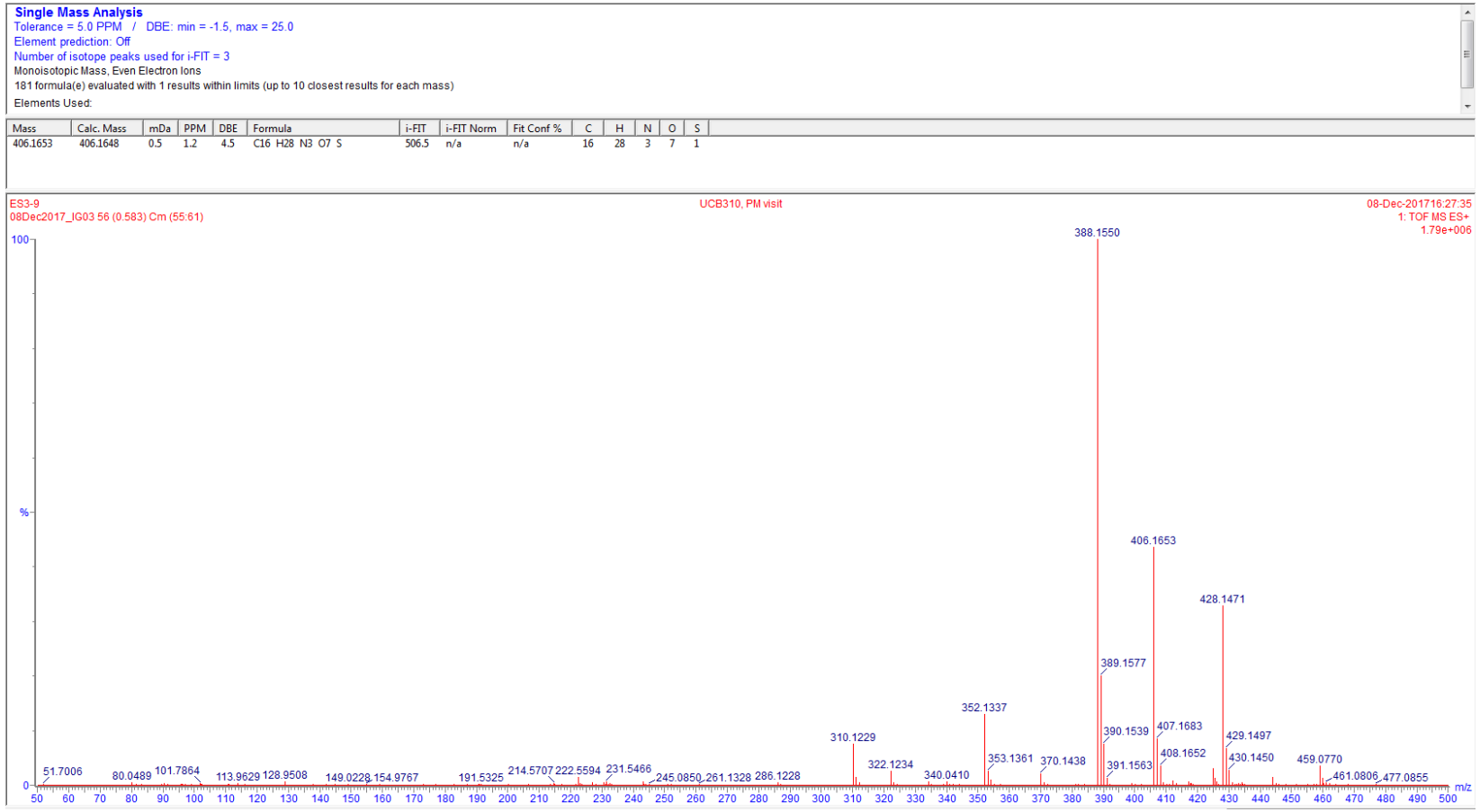

Figure A 2.15 HR-MS of Biotin-D-galactosamine **66**

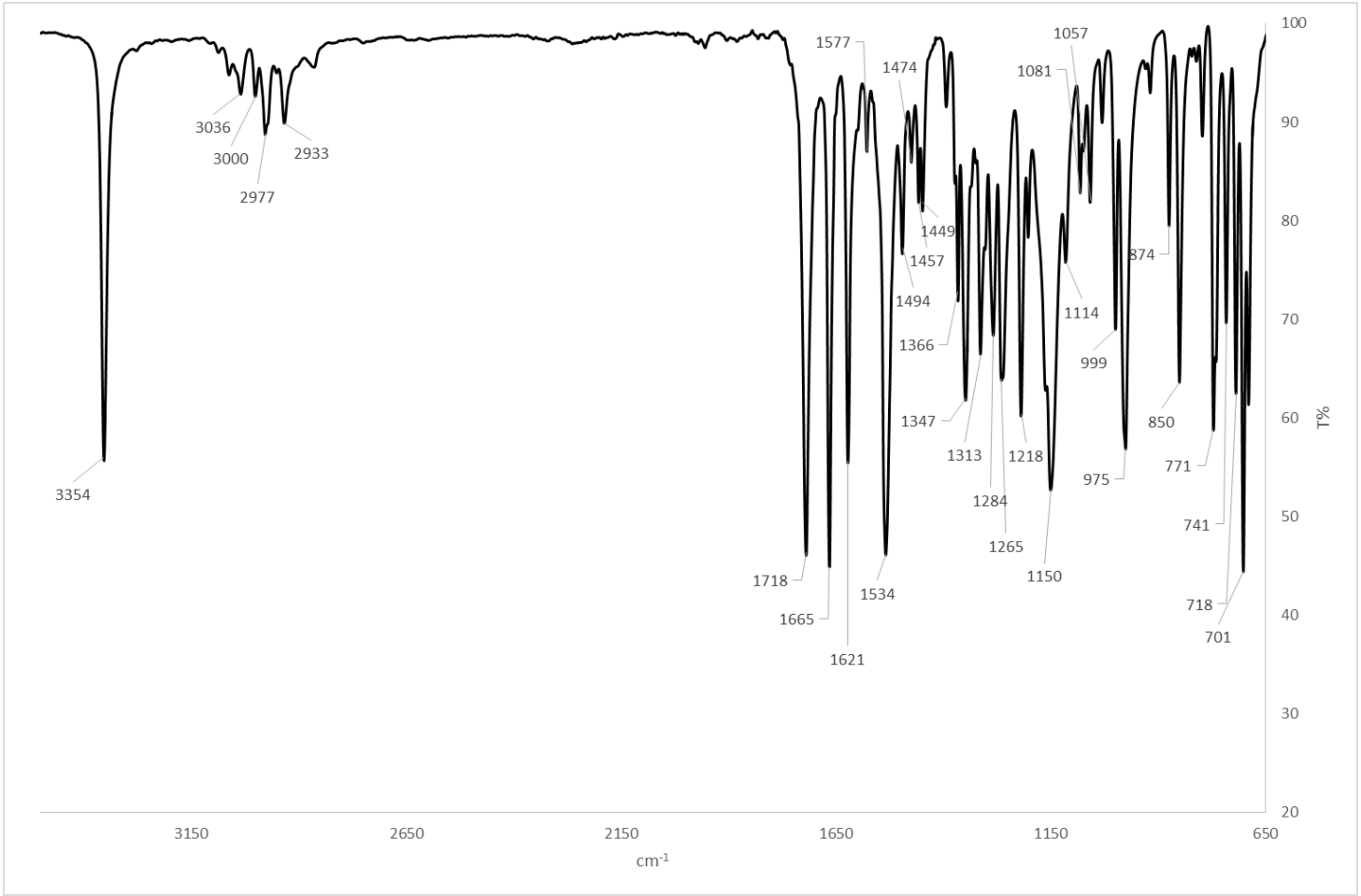

Figure A 2.16 IR spectrum (neat) of Cin-F-O*t*Bu **90**

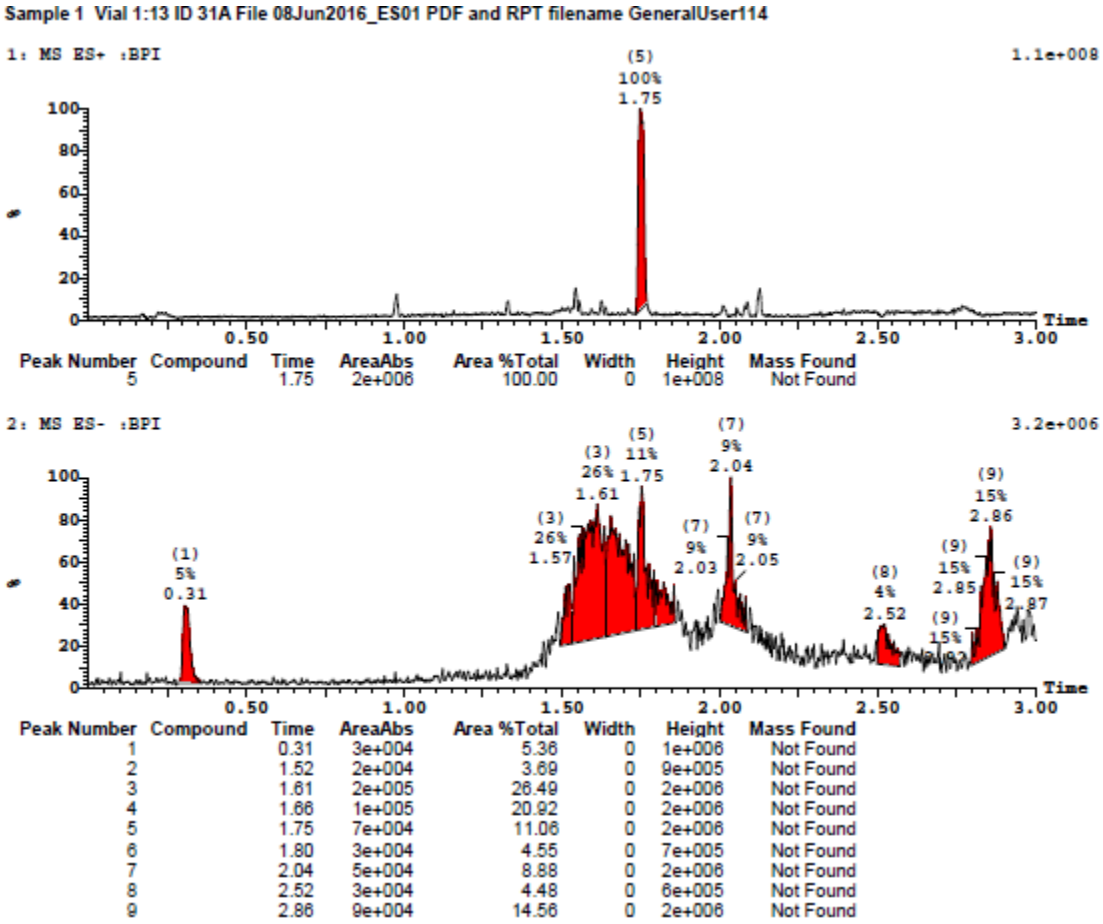

Figure A 2.17 MS (ES^+) of Cin-F-O*t*Bu ester **90**. Mass was not found

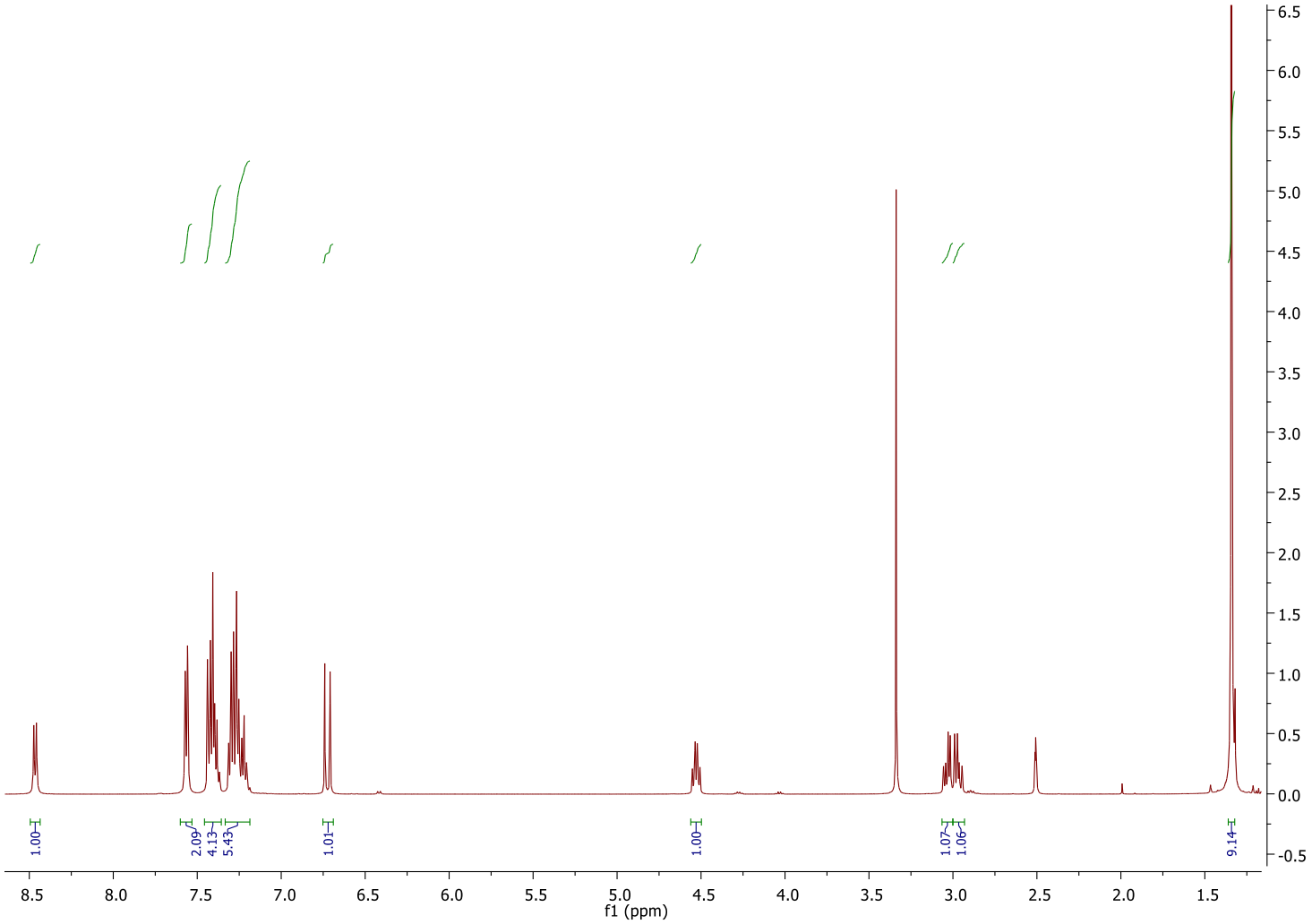

Figure A 2.18 ^{1}H NMR (500 MHz, dmso-d_6) of Cin-F-O*t*Bu **90**

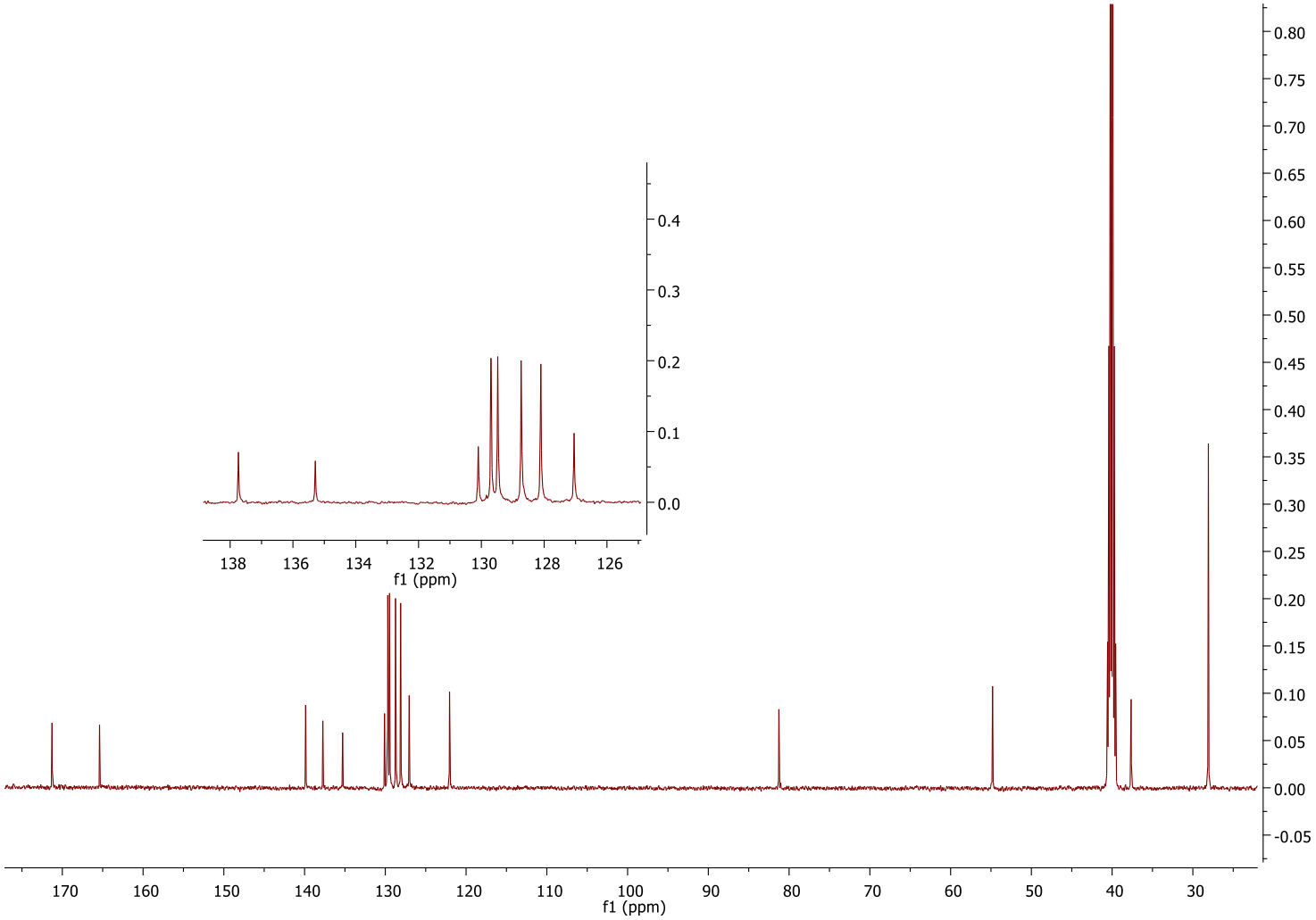

Figure A 2.19 ^{13}C NMR (126 MHz, dmso-d_6) of Cin-F-O*t*Bu **90**

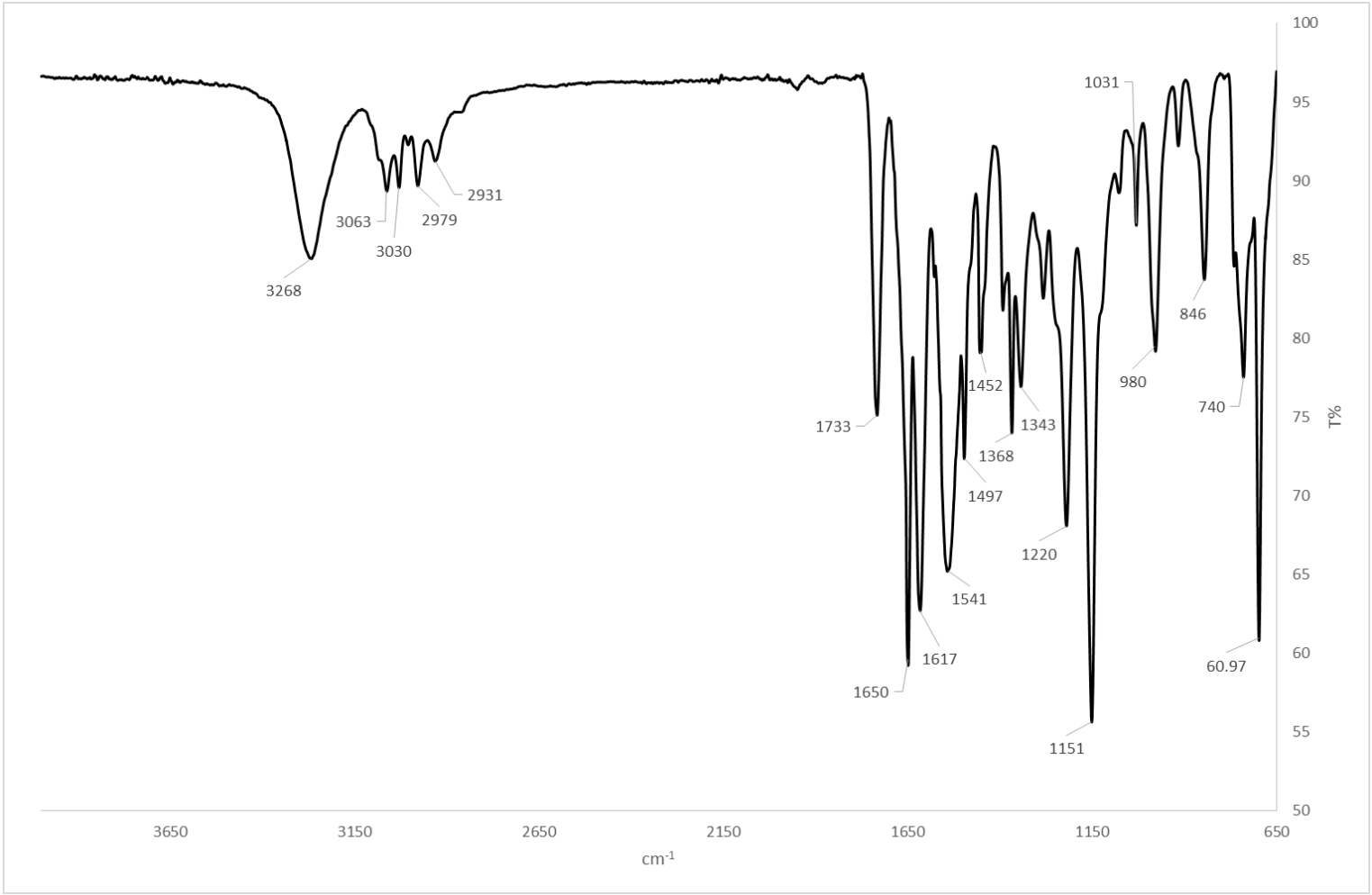

Figure A 2.20 IR spectrum (neat) of Cin-L-F-L-FO*t*Bu **91** and Cin-D-F-L-FO*t*Bu **92** mixture (2:1 ratio)

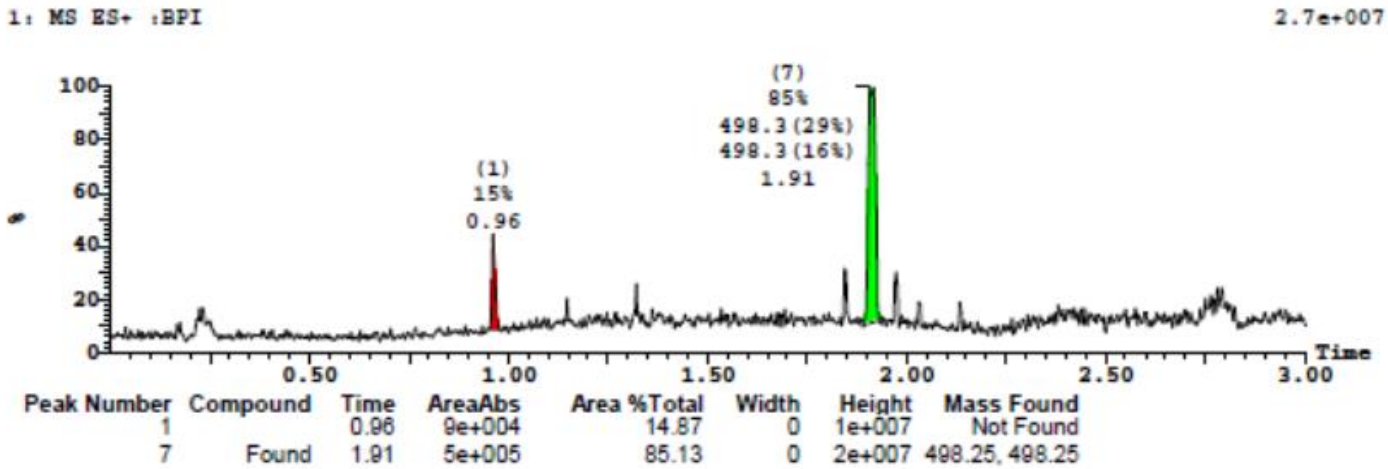

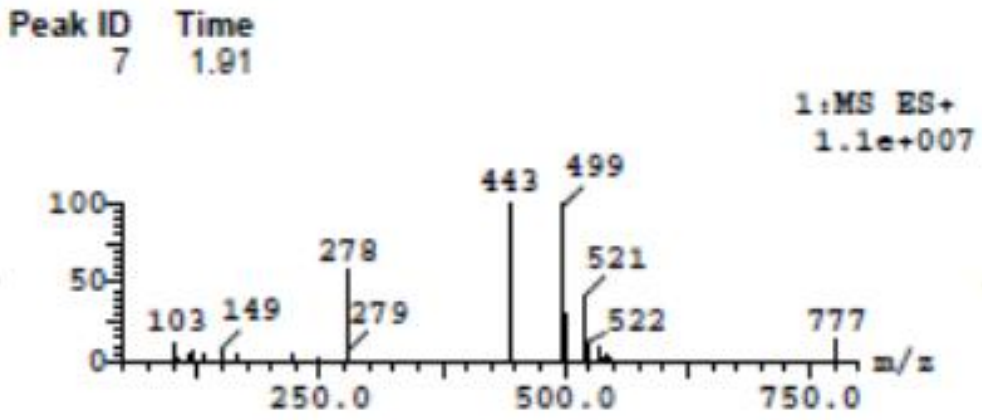

Figure A 2.21 MS (ES$^+$) of Cin-L-F-L-FO*t*Bu **91** and Cin-D-F-L-FO*t*Bu **92** mixture (2:1 ratio)

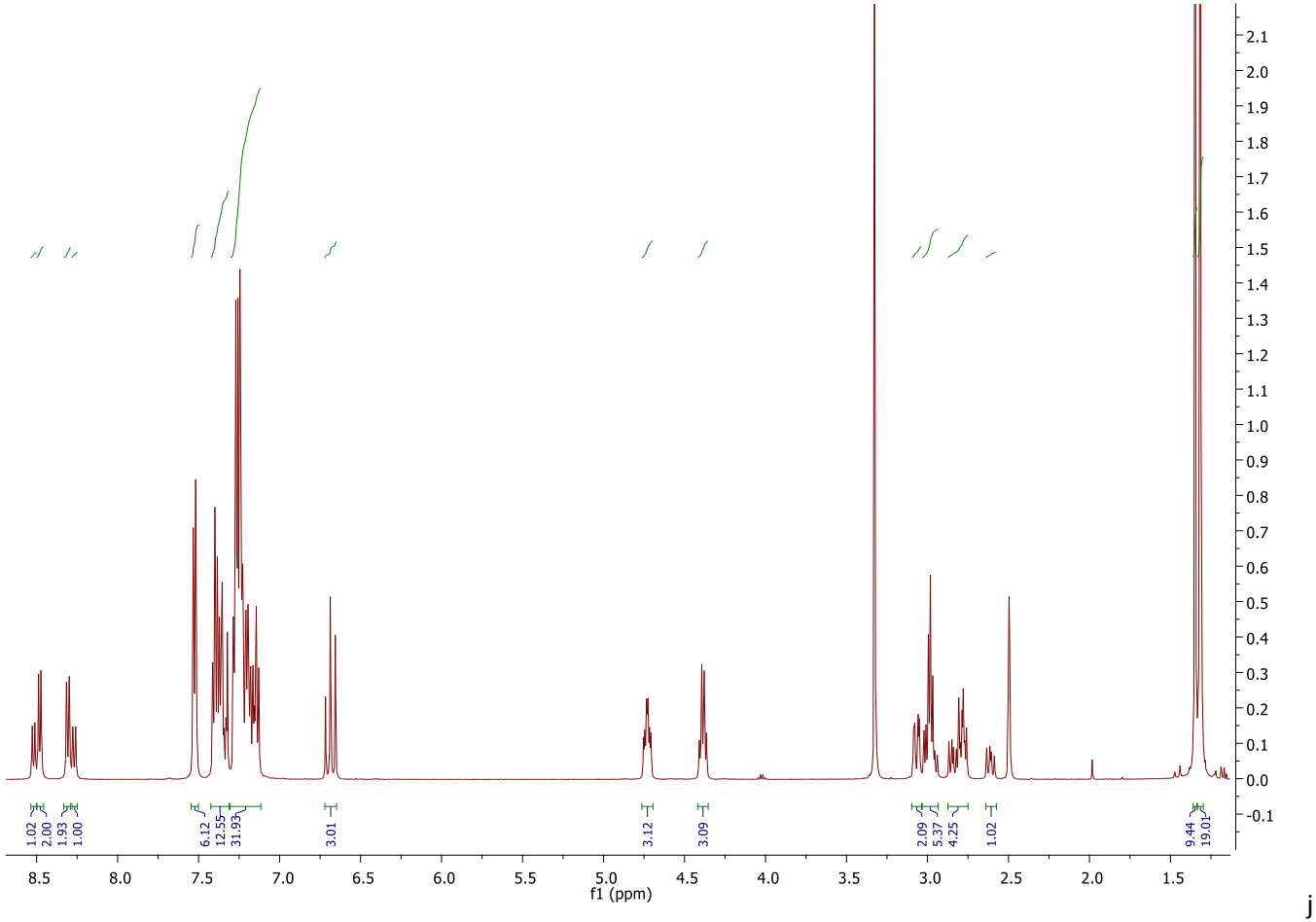

Figure A 2.22 ^{1}H NMR (500 MHz, dmso-d_6) spectrum of Cin-L-F-L-FO*t*Bu **91** and Cin-D-F-L-FO*t*Bu **92** mixture (2:1 ratio)

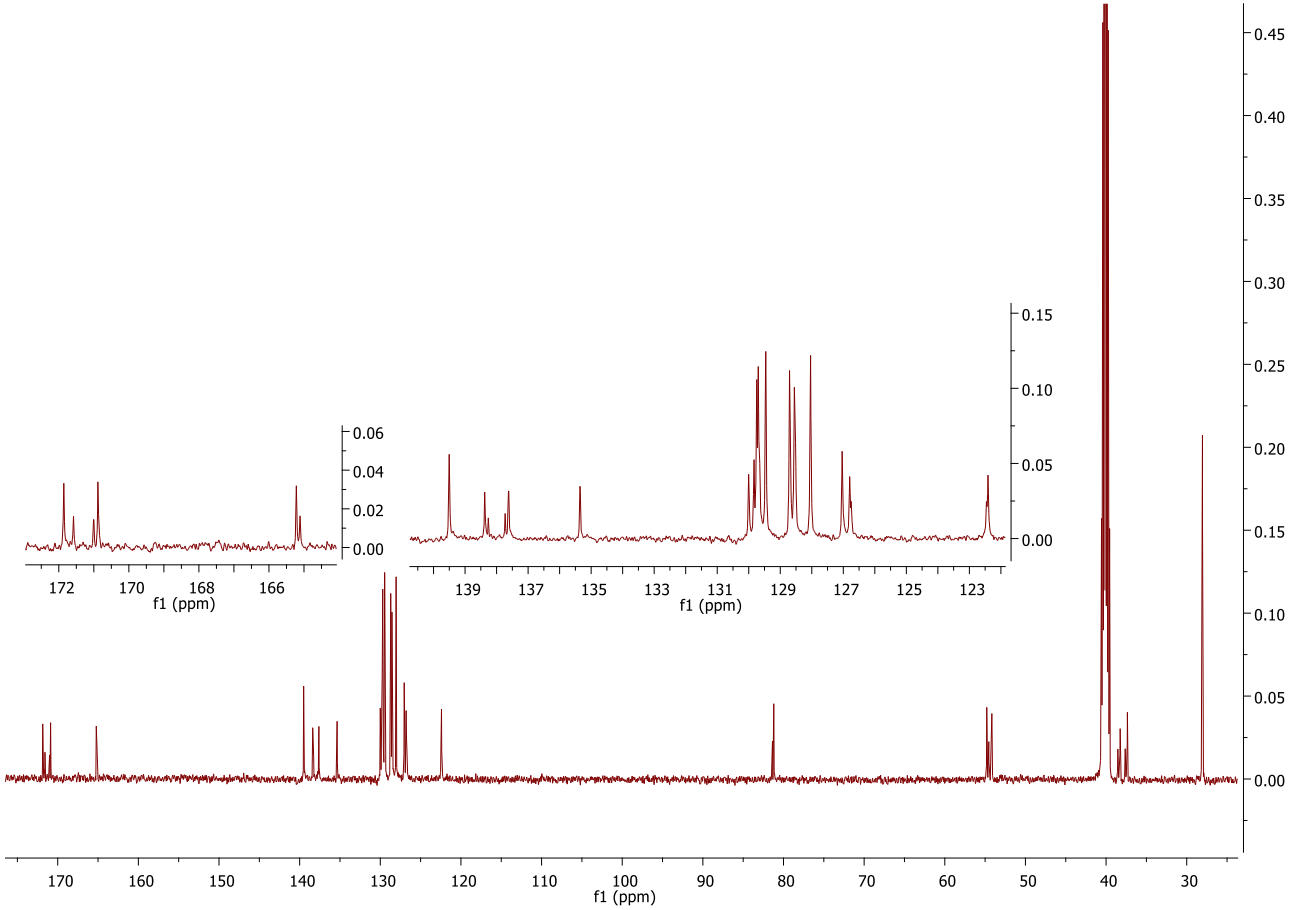

Figure A 2.23 ^{13}C NMR (126 MHz, dmso-d_6) spectrum of Cin-L-F-L-FO*t*Bu **91** and Cin-D-F-L-FO*t*Bu **92** mixture (2:1 ratio)

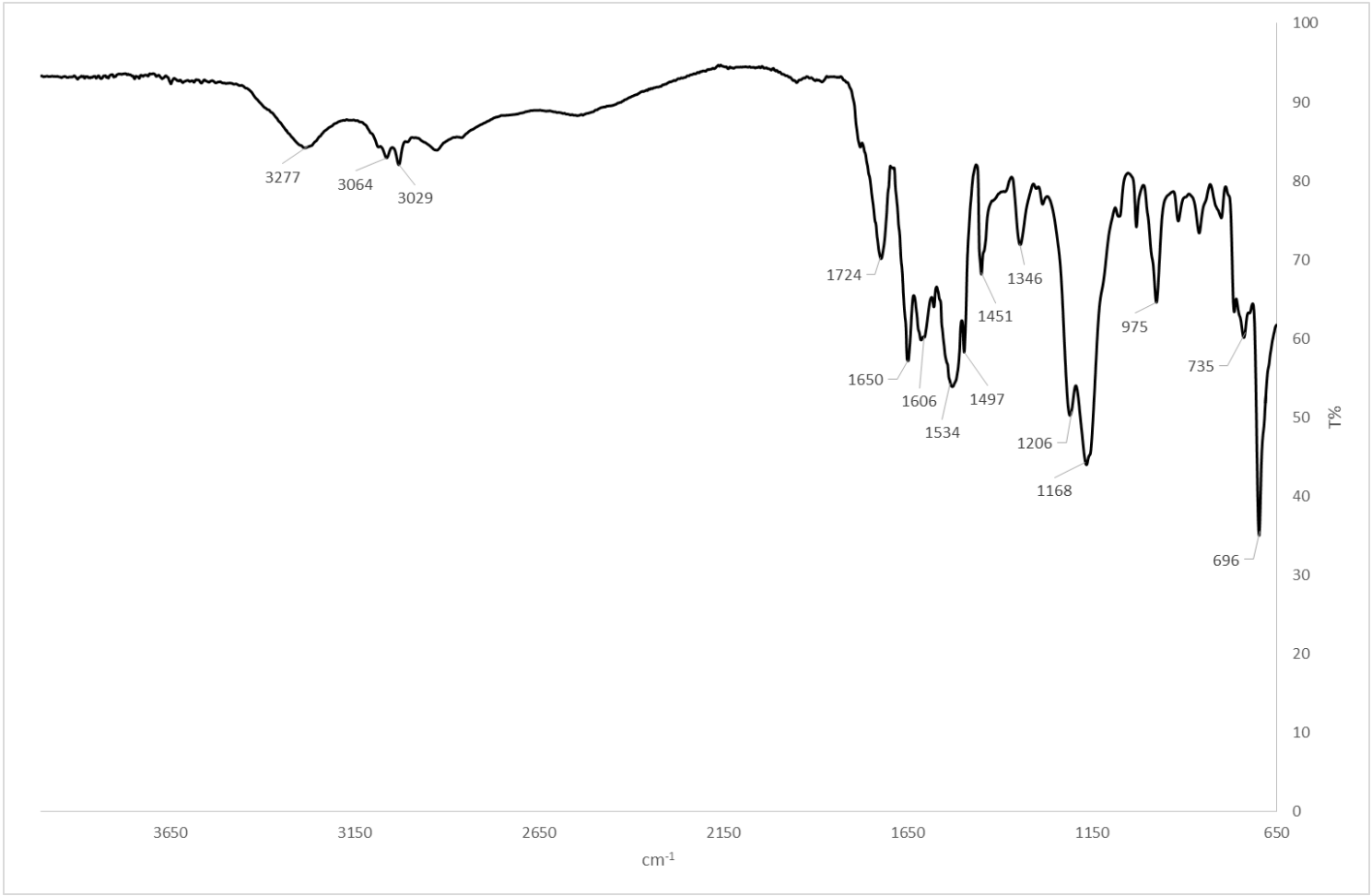

Figure A 2.24 IR spectrum (neat) of Cin-L-F-L-F **70** and Cin-D-F-L-F **93** mixture (2:1 ratio)

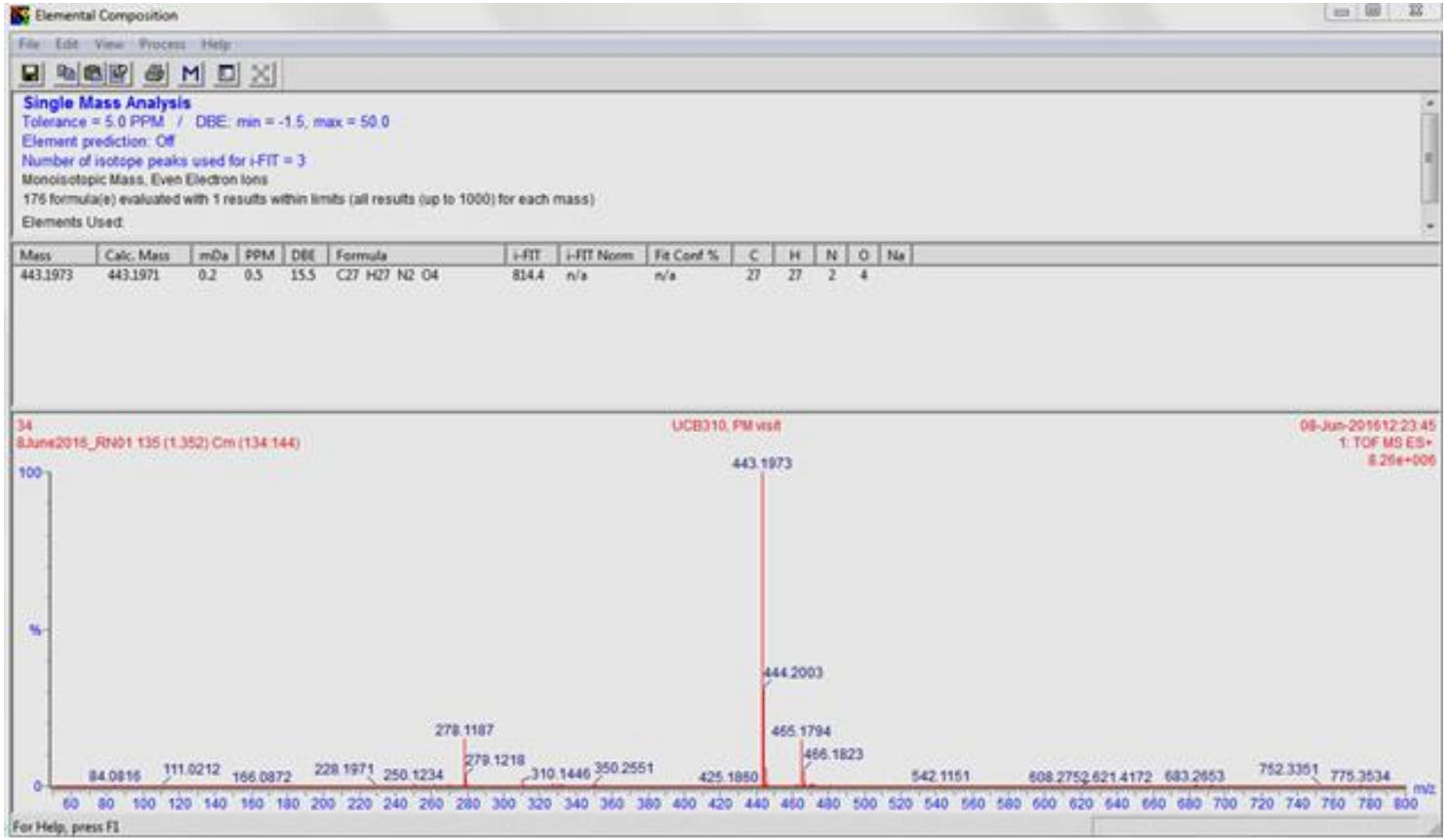

Figure A 2.25 HR-MS $[M+H]^+$of Cin-L-F-L-F **70** and Cin-D-F-L-F **93** mixture (2:1 ratio)

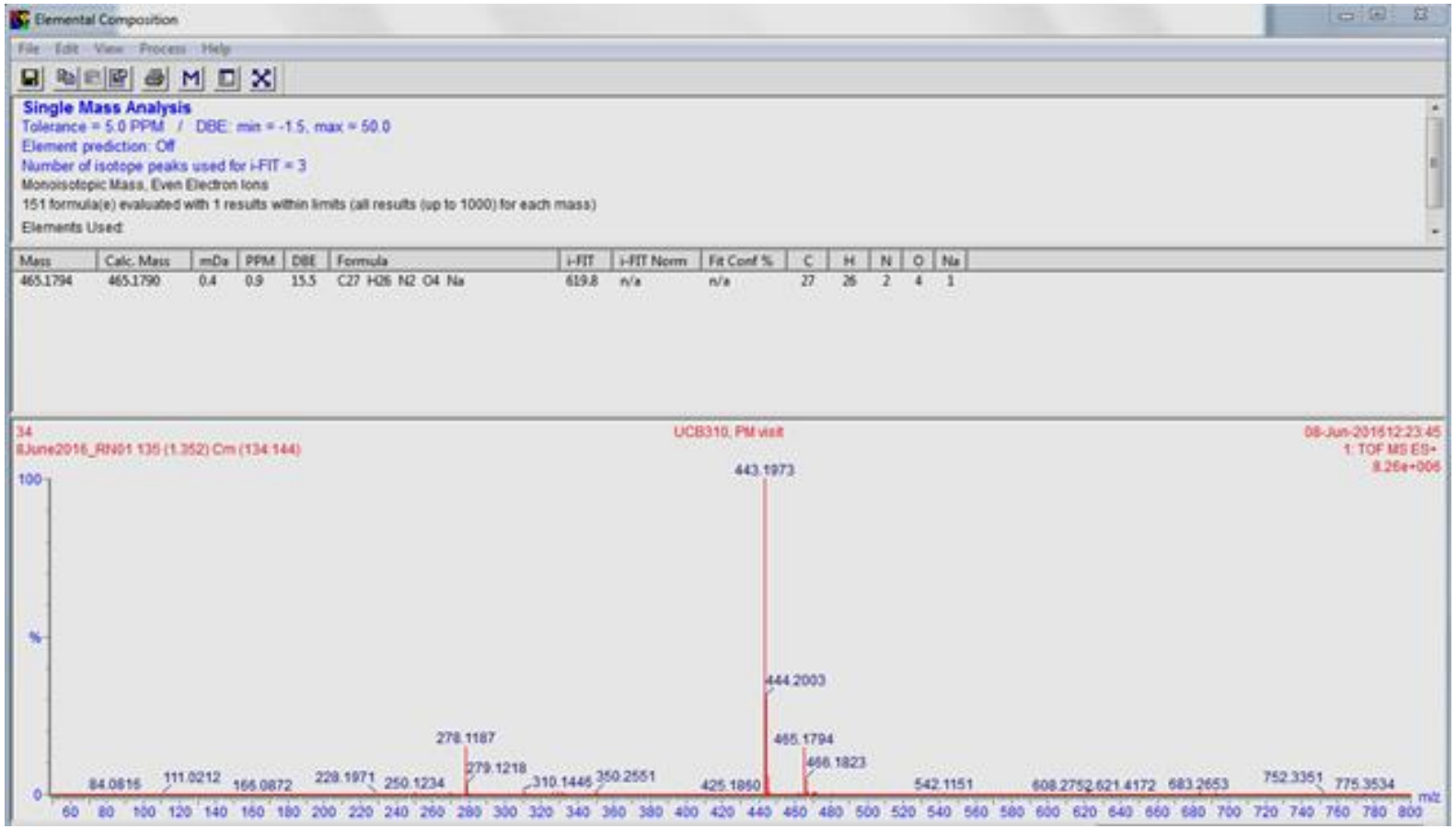

Figure A 2.26 HR-MS $[M+Na]^+$ of Cin-L-F-L-F **70** and Cin-D-F-L-F **93** mixture (2:1 ratio)

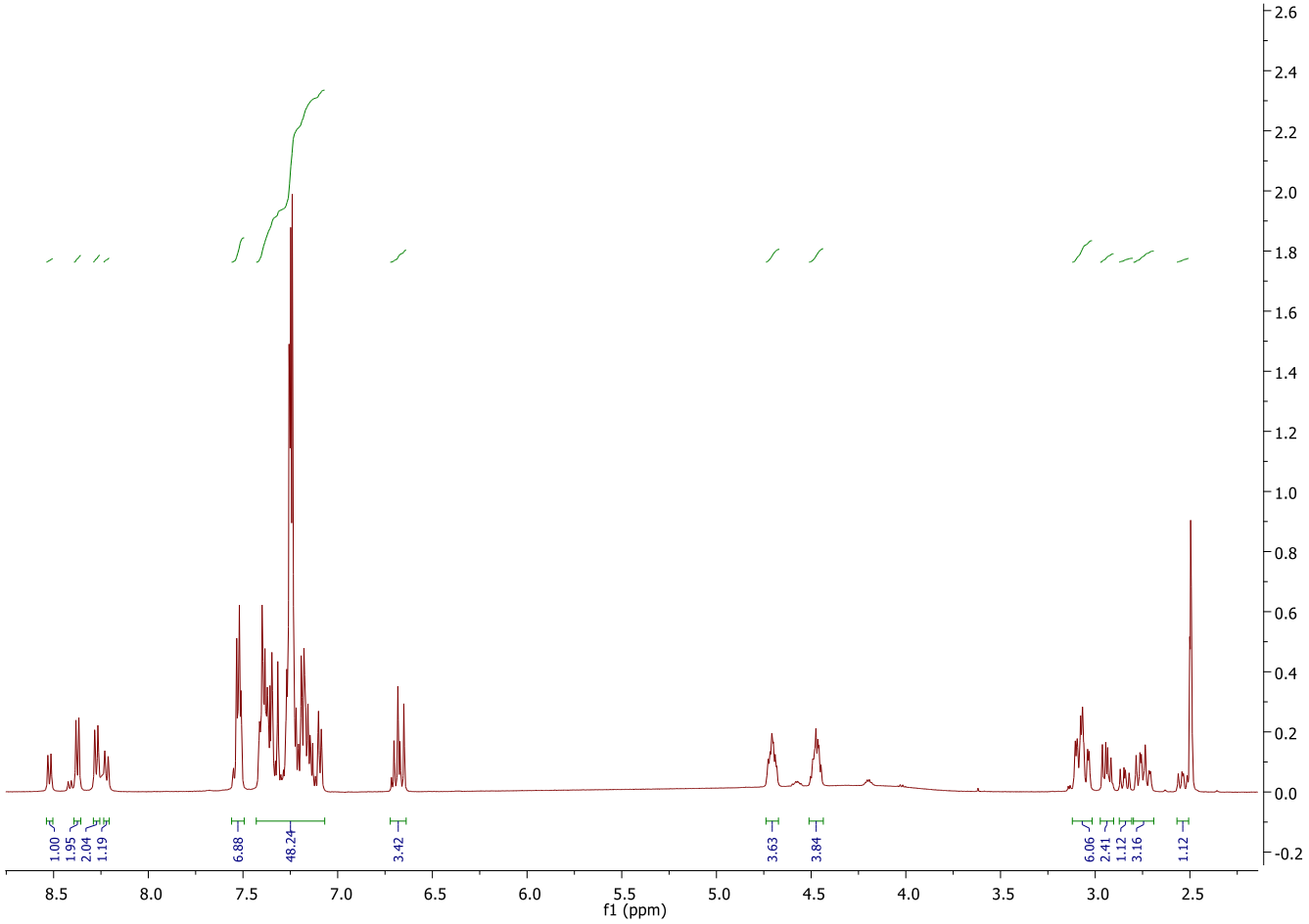

Figure A 2.27 ^{1}H NMR (500 MHz, dmso-d_6) spectrum of Cin-L-F-L-F **70** and Cin-D-F-L-F **93** mixture (2:1 ratio)

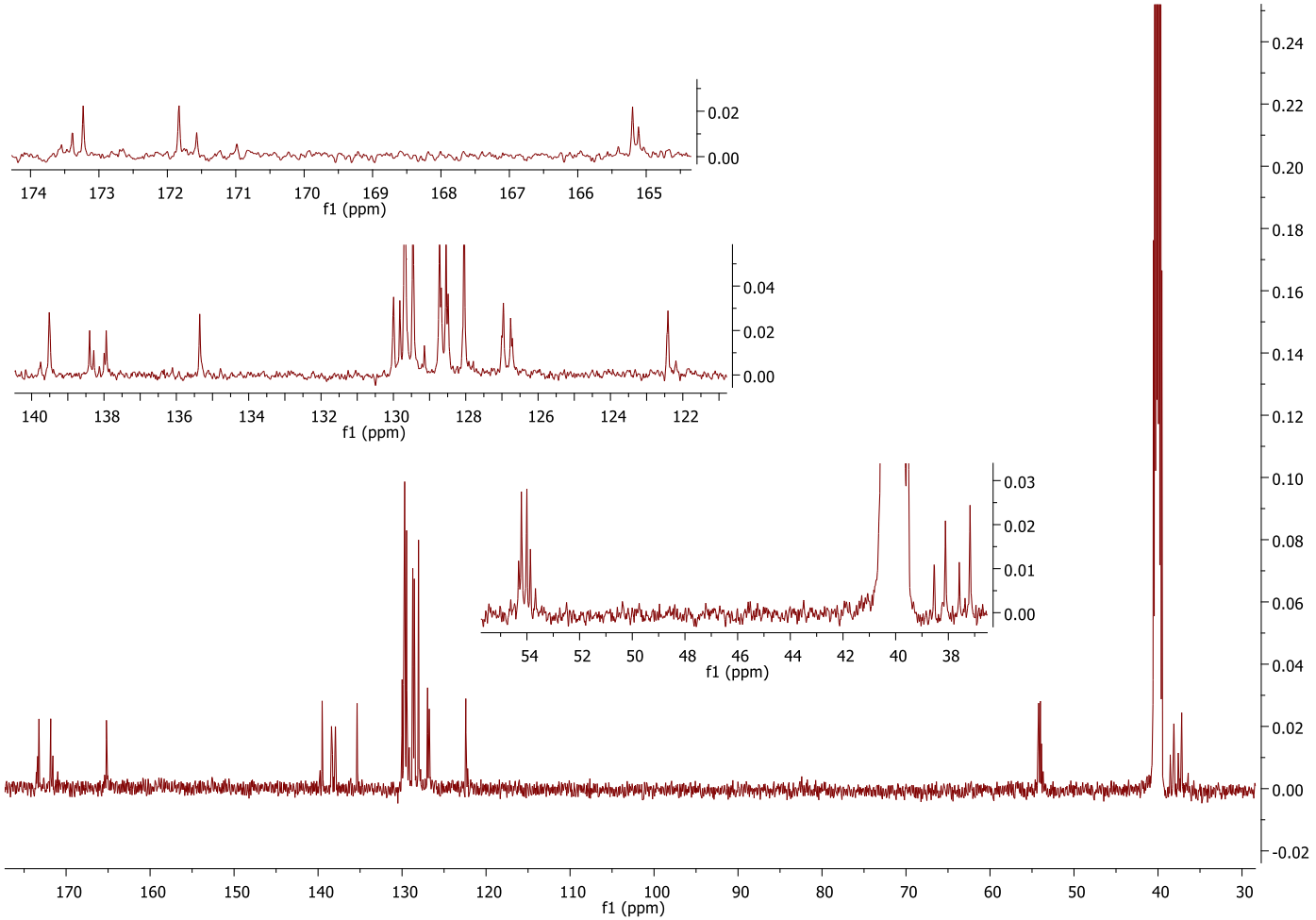

Figure A 2.28 ^{13}C NMR (126 MHz, dmso-d_6) spectrum of Cin-L-F-L-F **70** and Cin-D-F-L-F **93** mixture (2:1 ratio)

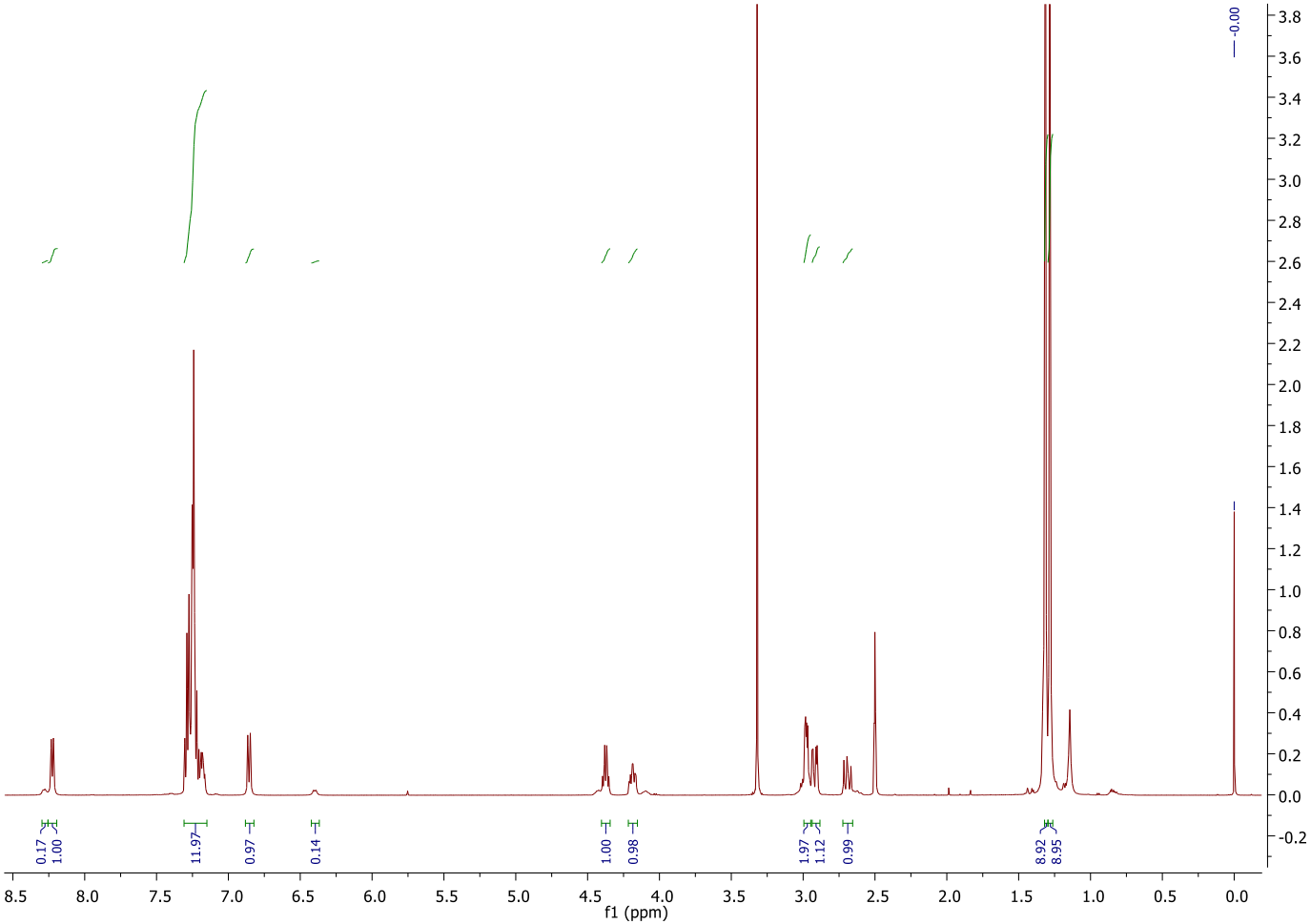

Figure A 2.29 ^{1}H NMR (500 MHz, dmso-d_6) spectrum of *Boc*-F-FO*t*Bu **102**

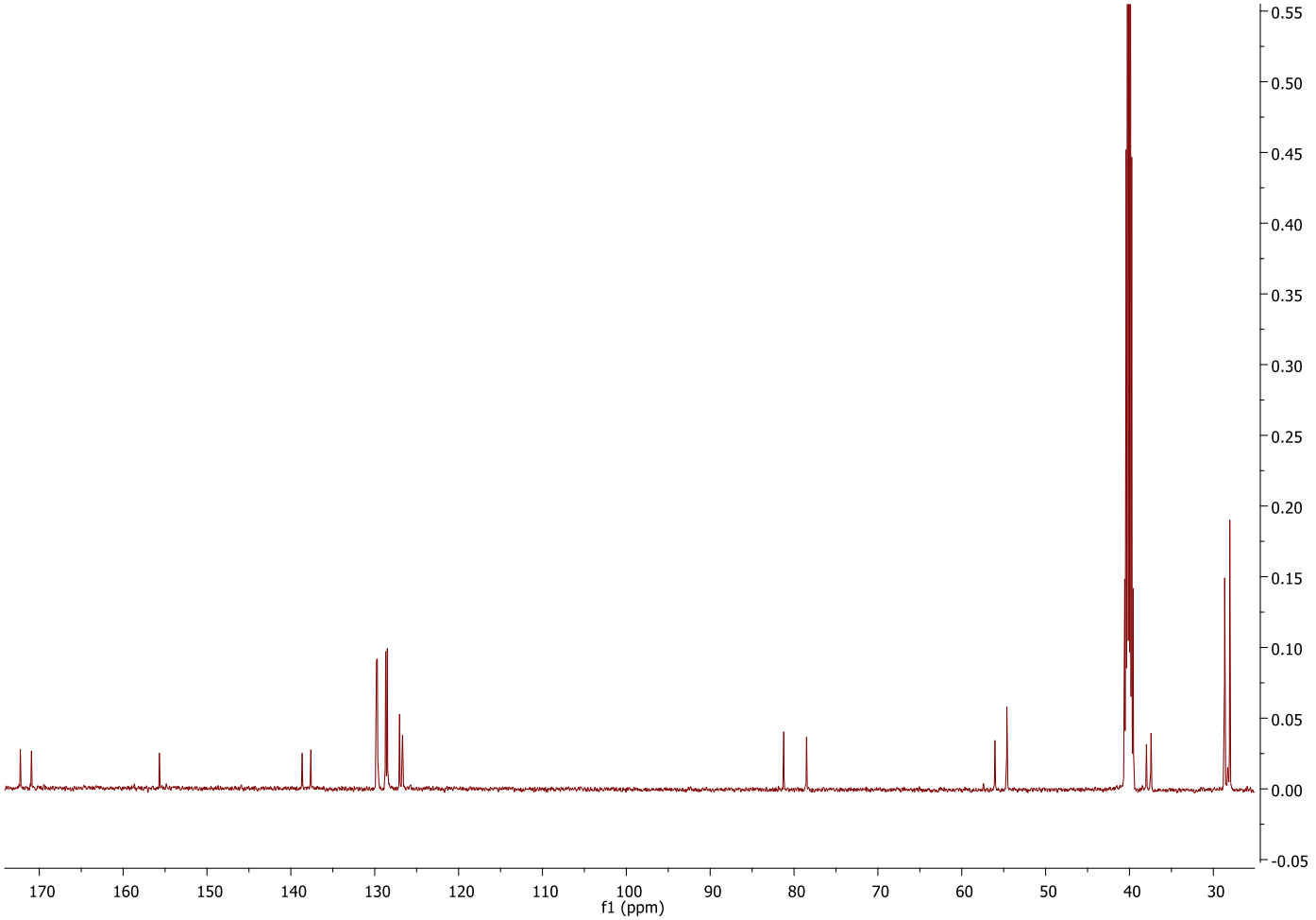

Figure A 2.30 ^{13}C NMR (126 MHz, dmso-d_6) spectrum of *Boc*-F-FO*t*Bu **102**

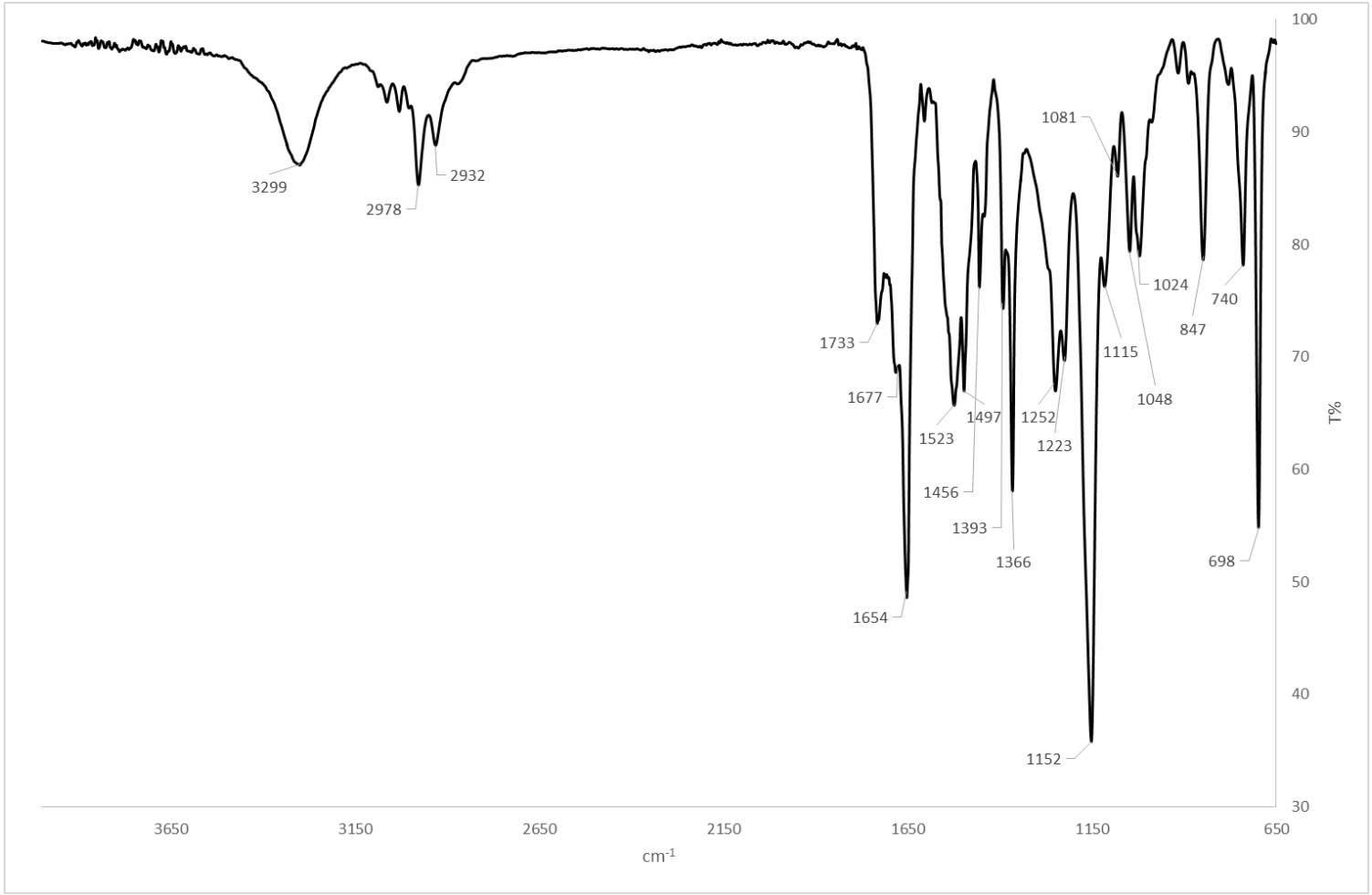

Figure A 2.31 IR spectrum (neat) of *Boc*-F-FO*t*Bu **102**

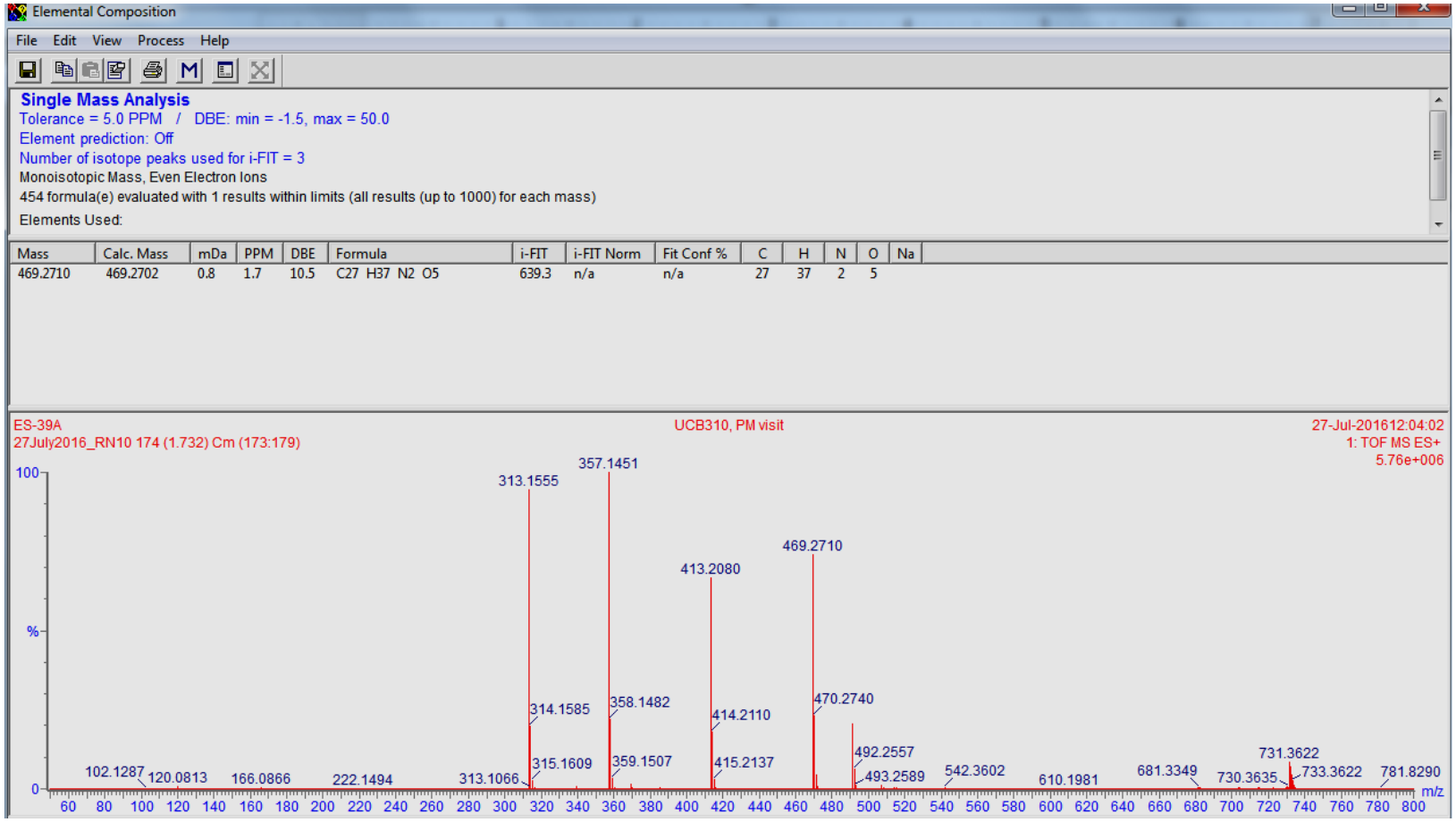

Figure A 2.32 HR MS $[M+H]^+$ of *Boc*-F-FO*t*Bu **102**. Mass found m/z 491 (tentative)

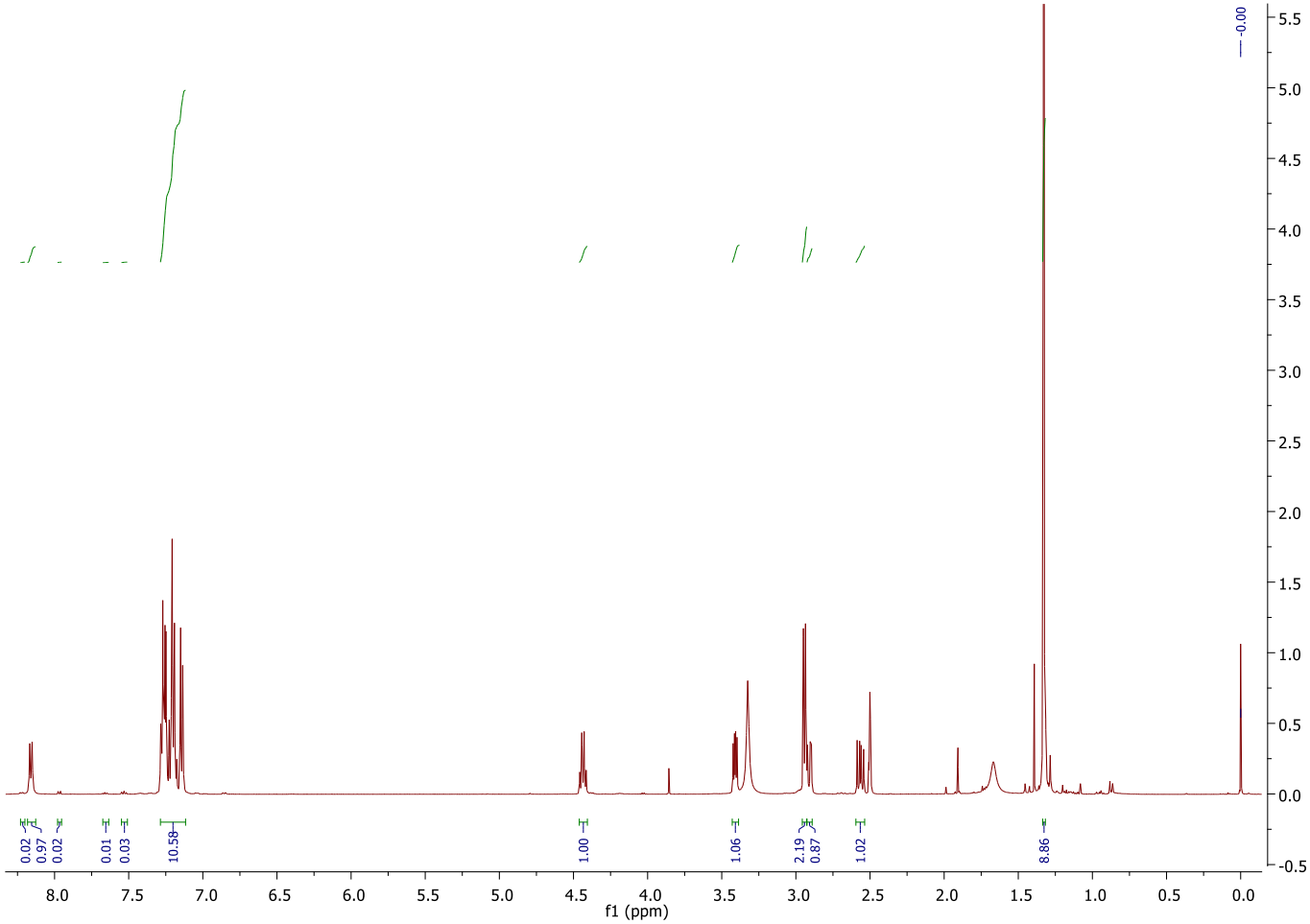

Figure A 2.33 ^{1}H NMR (500 MHz, dmso-d_6) spectrum of F-FO*t*Bu **103**

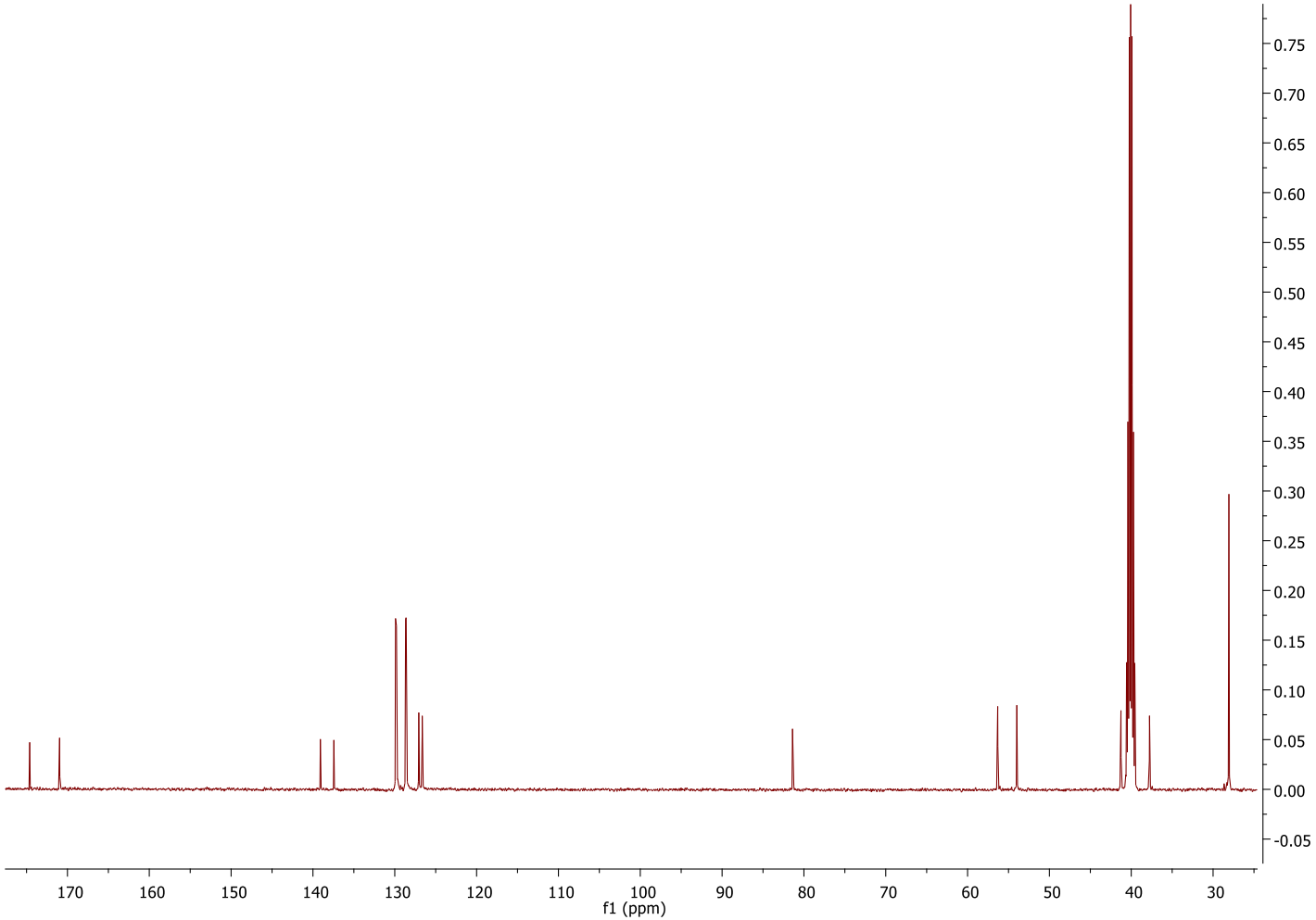

Figure A 2.34 ^{13}C NMR (126 MHz, dmso-d_6) spectrum of F-FO*t*Bu **103**

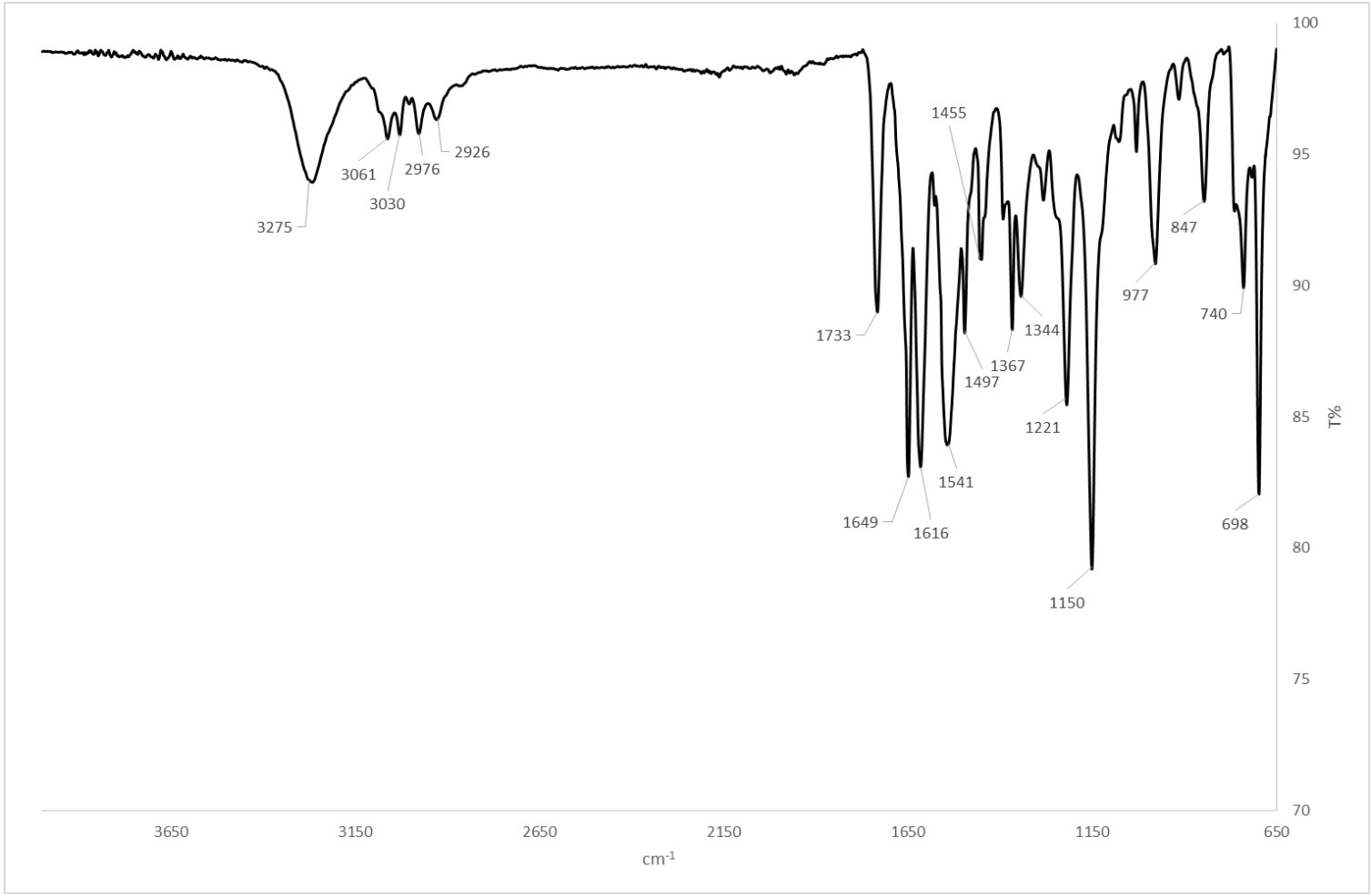

Figure A 2.35 IR spectrum (neat) of Cin-F-FO*t*Bu **91**

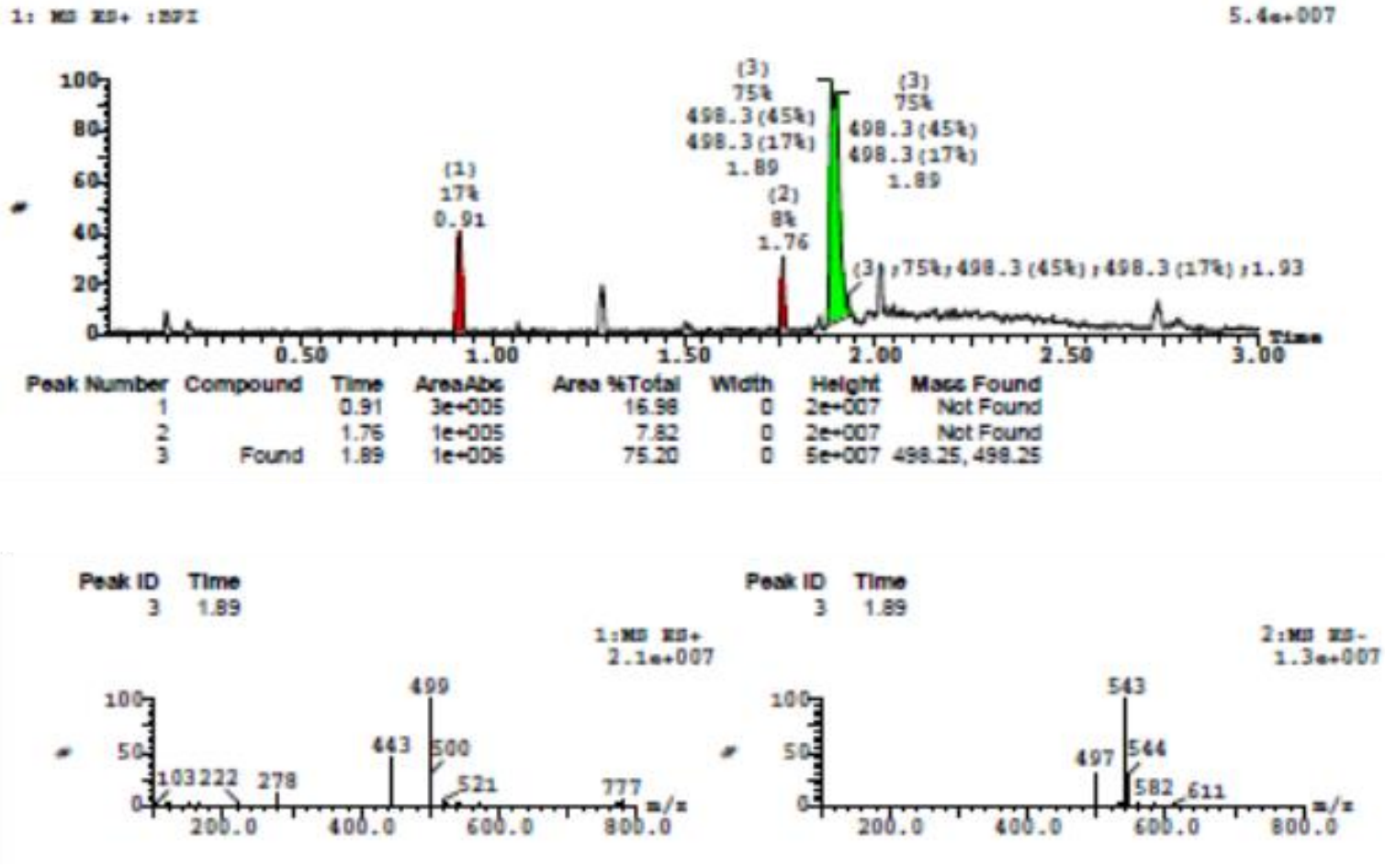

Figure A 2.36 MS (ES^+) and (ES^-): of Cin-F-FO*t*Bu **91**

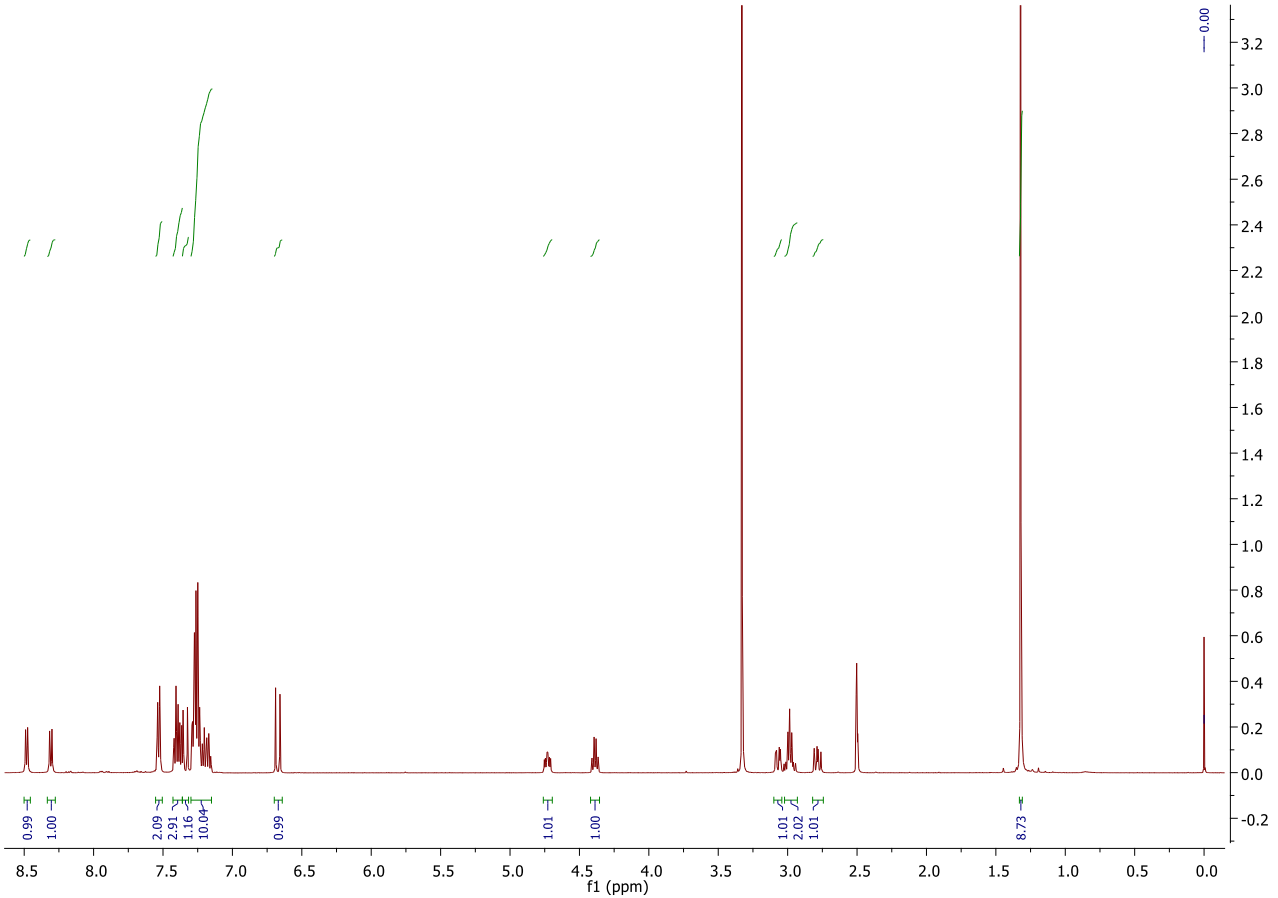

Figure A 2.37 ^{1}H NMR (500 MHz, dmso-d_6) spectrum of Cin-F-FO*t*Bu **91**

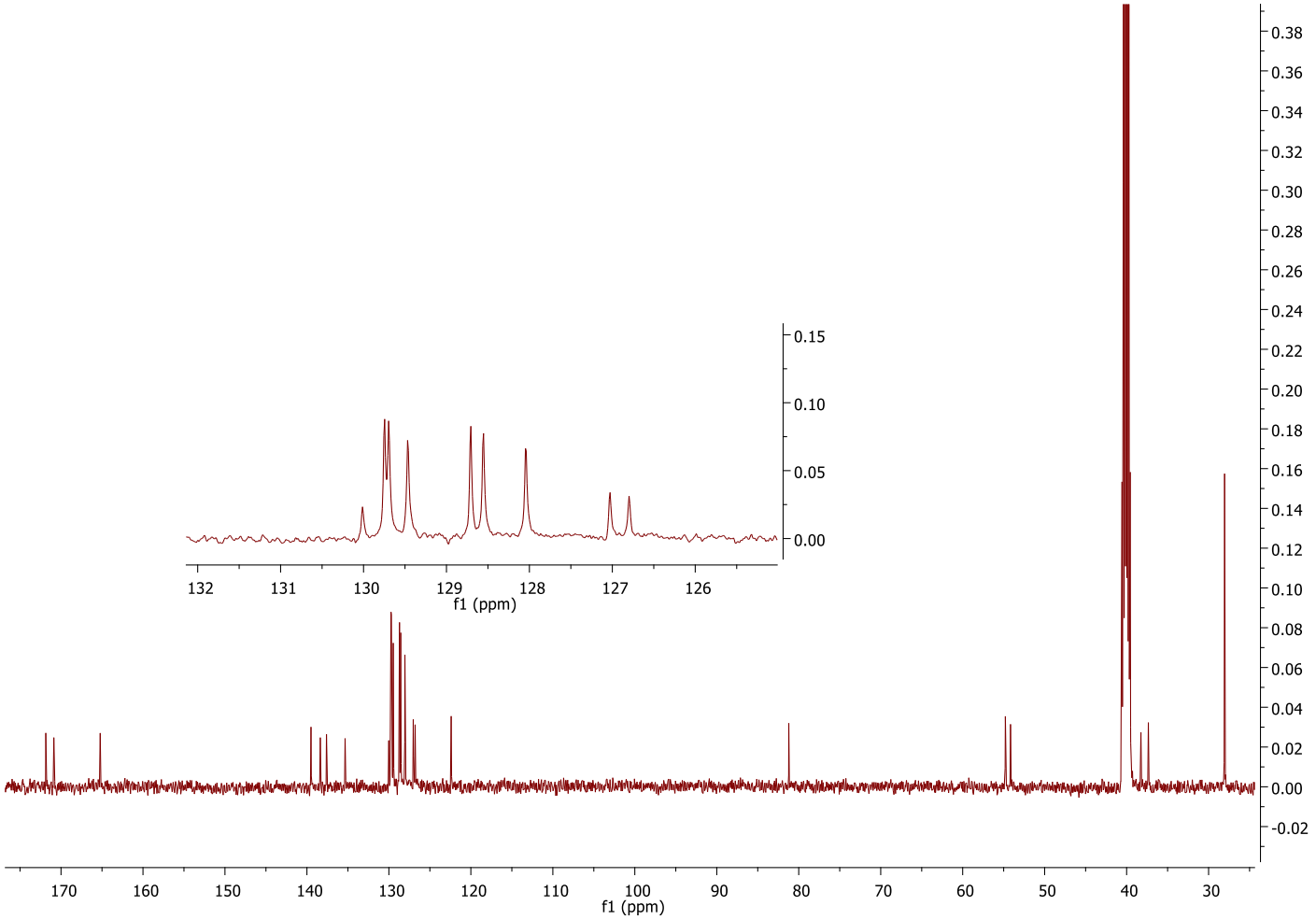

Figure A 2.38 ^{13}C NMR (126 MHz, dmso-d_6) spectrum of Cin-F-FO*t*Bu **91**

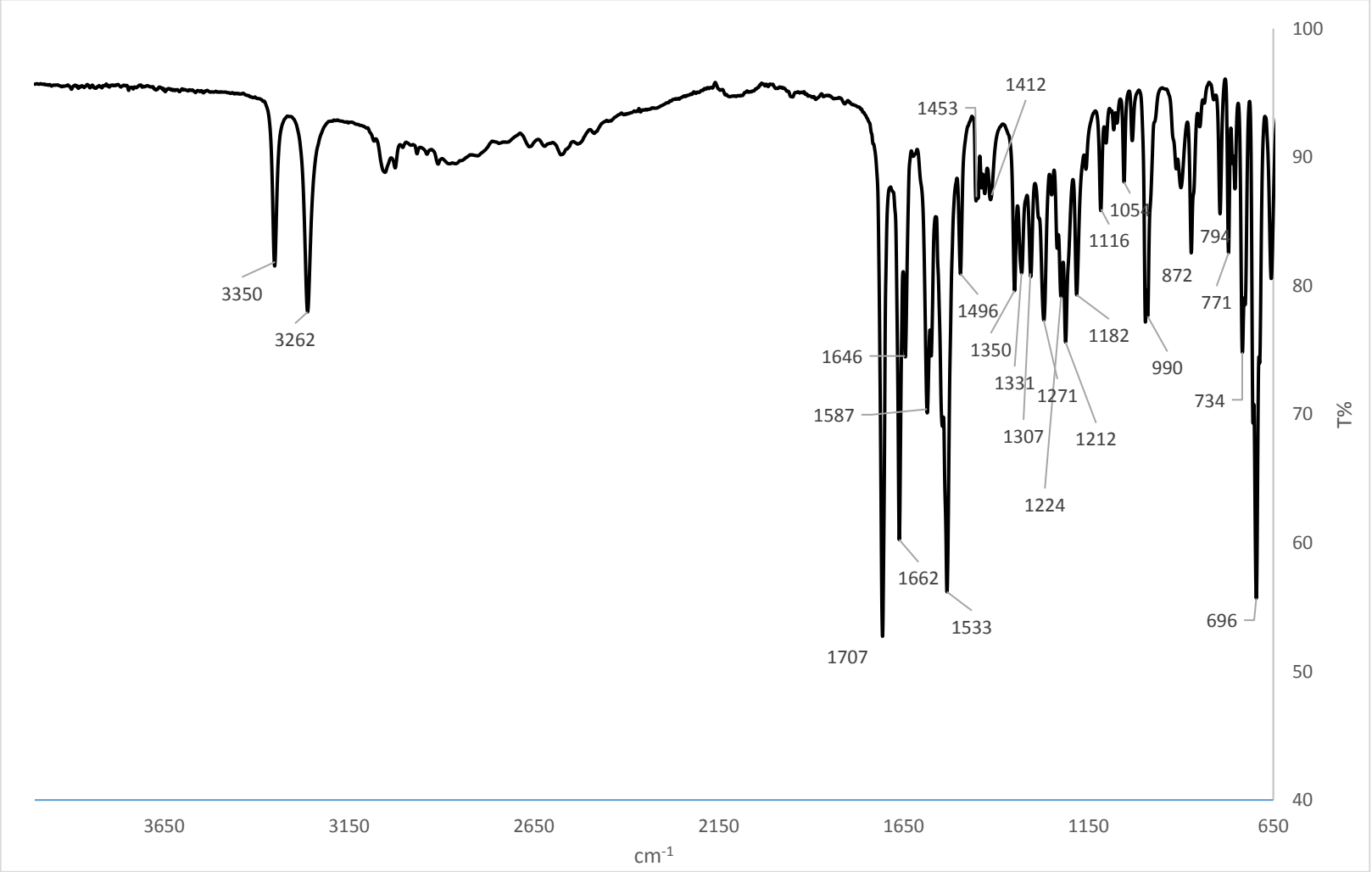

Figure A 2.39 IR (neat) of Cin-F-F **70**

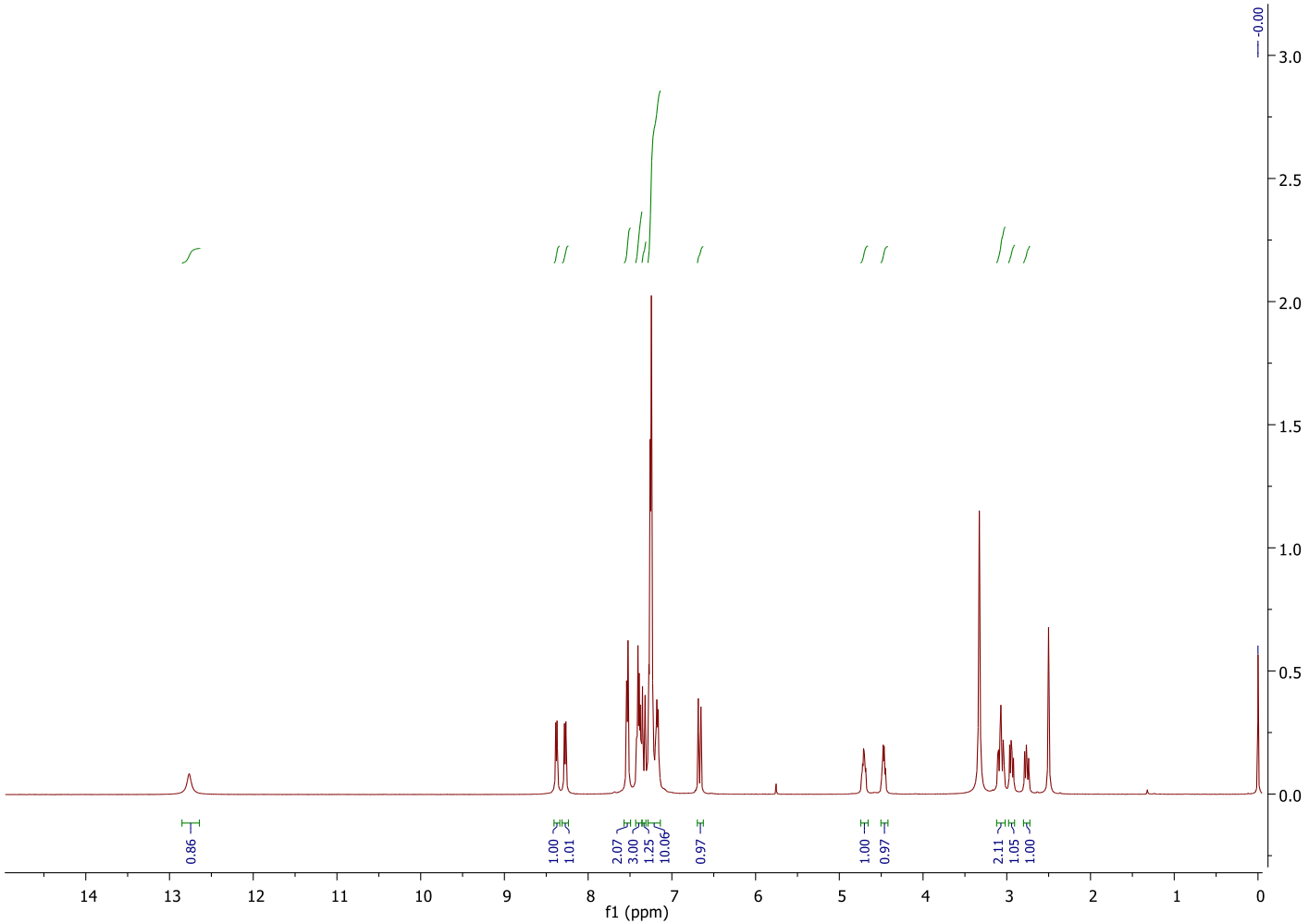

Figure A 2.40 ^{1}H NMR (500 MHz, dmso-d_6) spectrum of Cin-F-F **70**

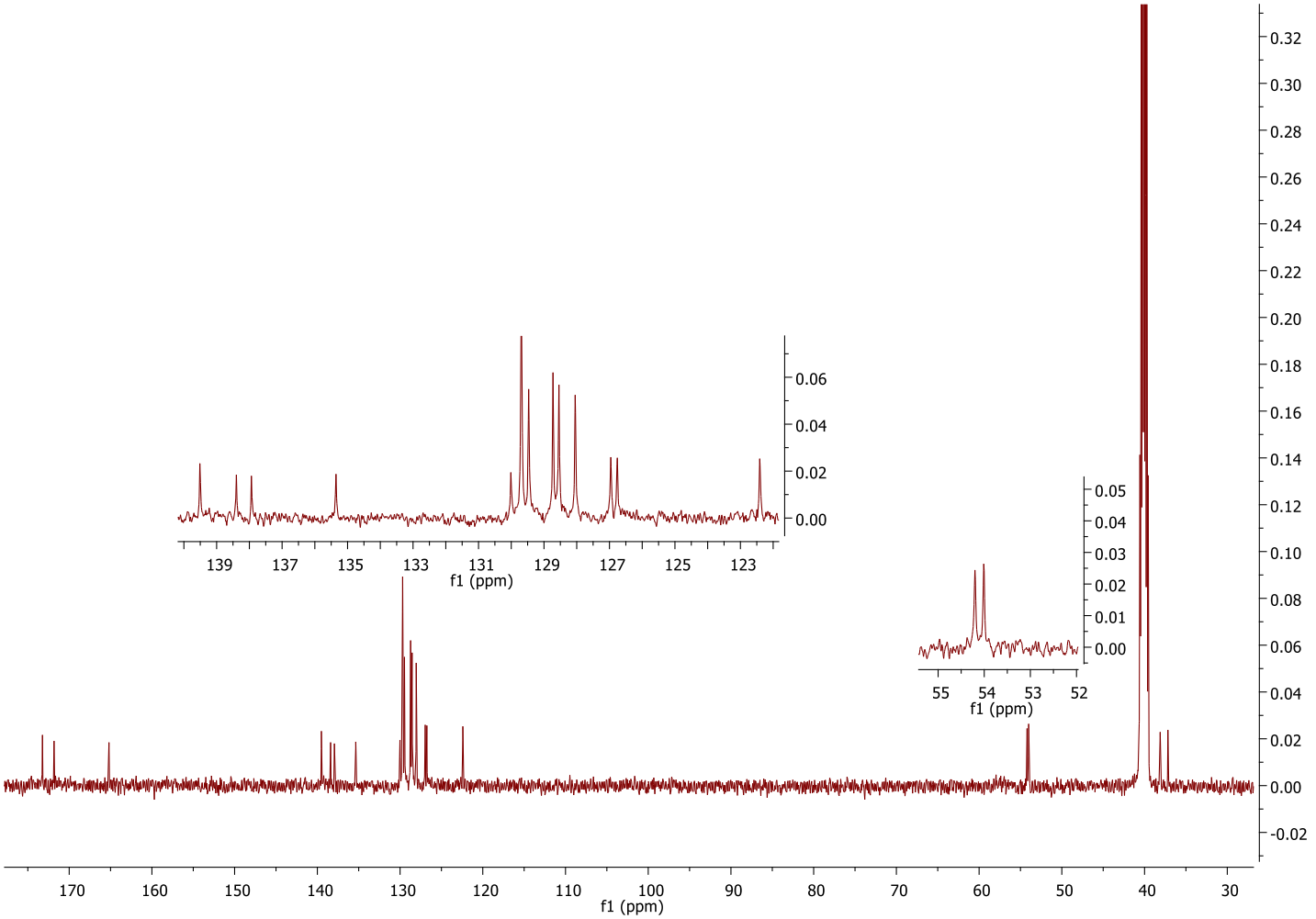

Figure A 2.41 ^{13}C NMR (126 MHz, dmso-d_6) spectrum of Cin-F-F **70**

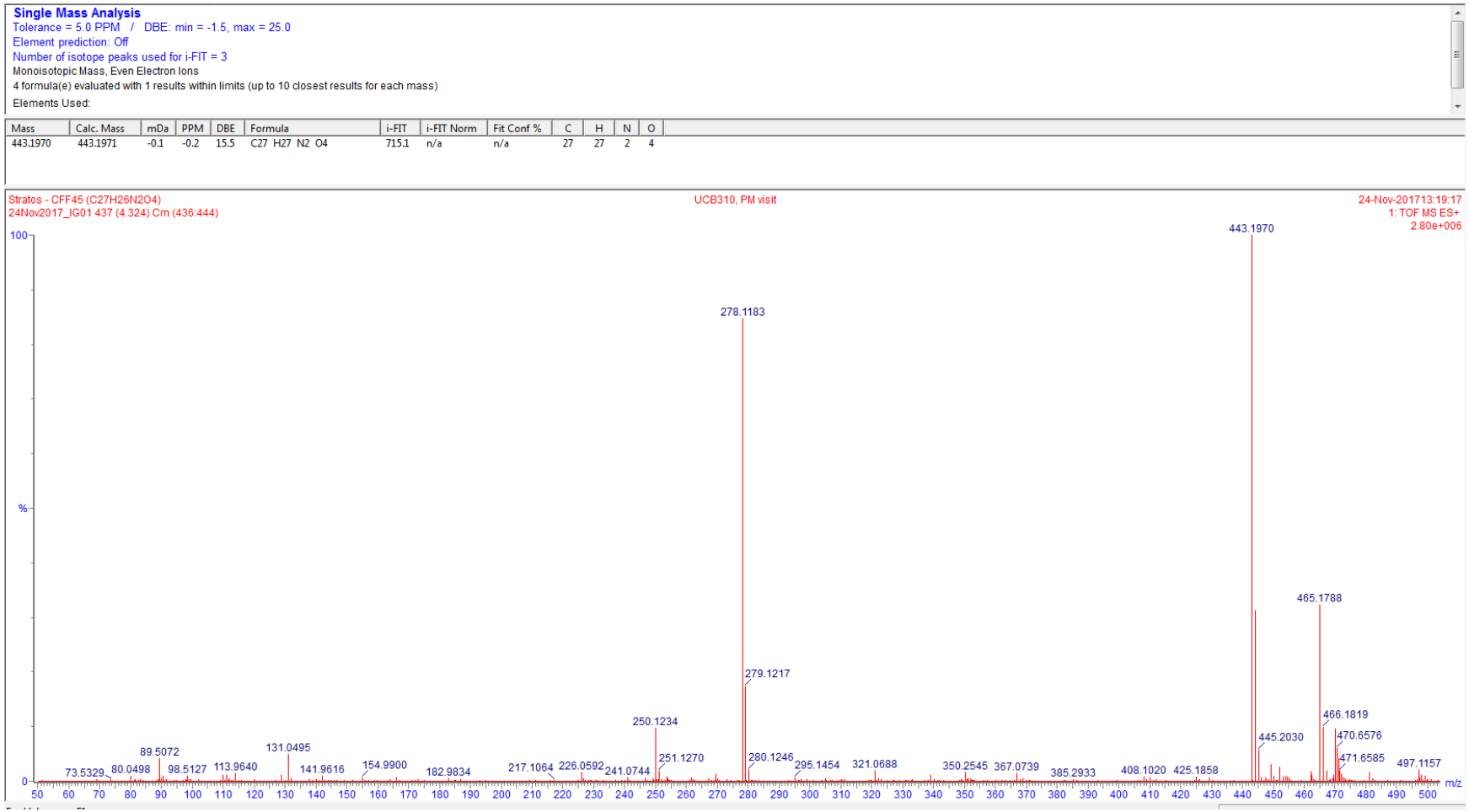

Figure A 2.42 HR-MS of Cin-F-F **70**

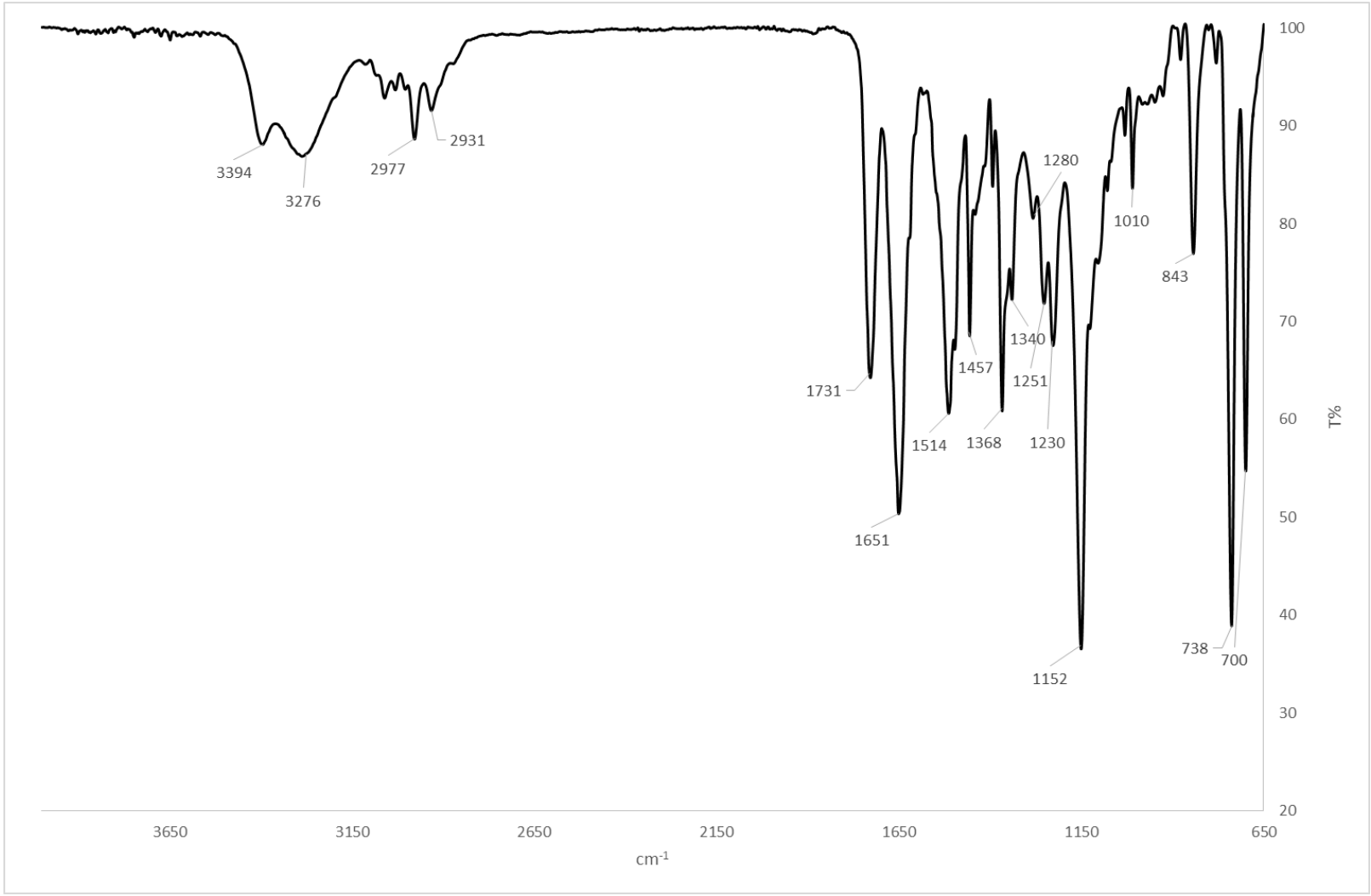

Figure A 2.43 IR spectrum (neat) of Ind-FO*t*Bu **108**

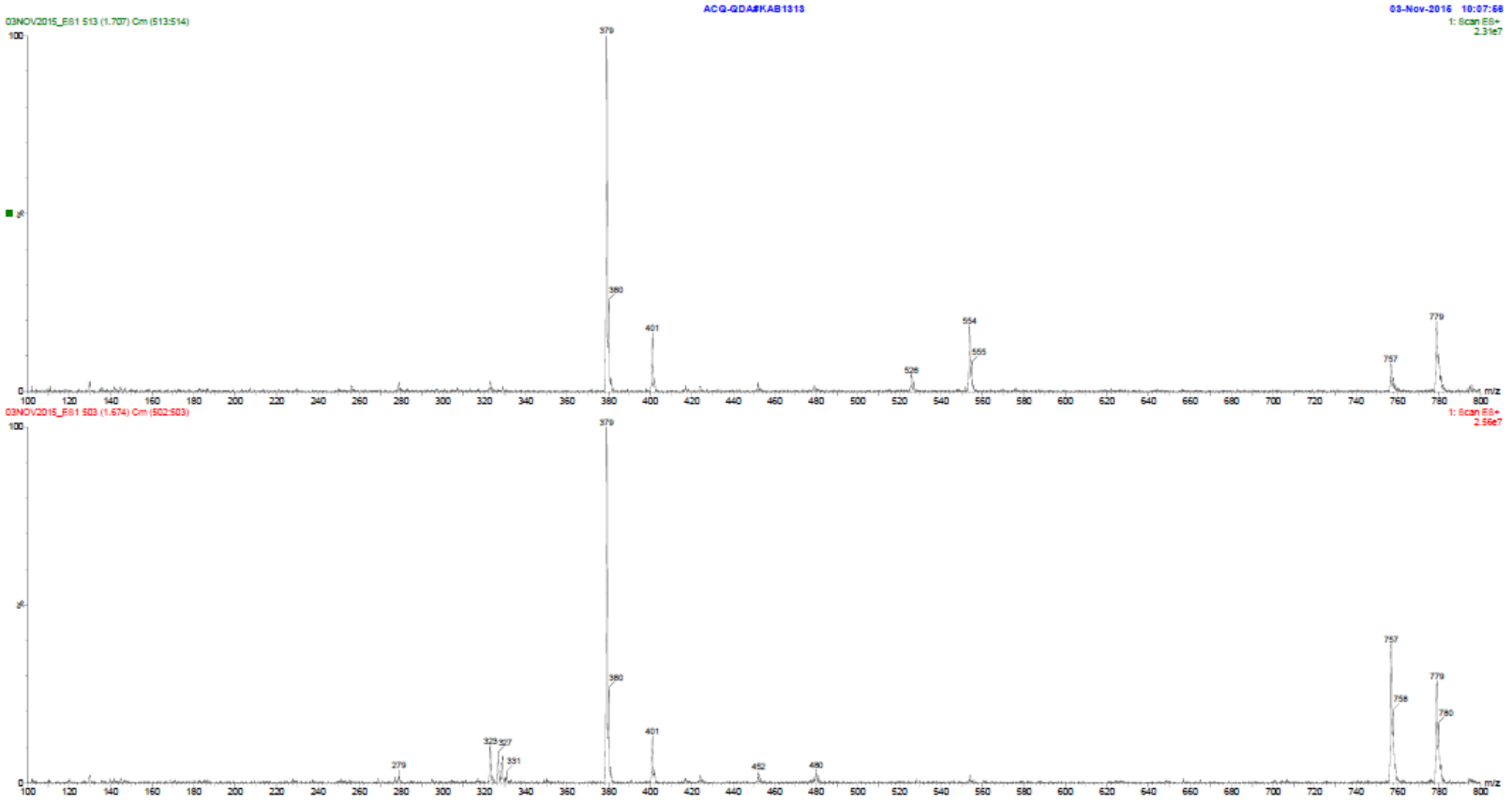

Figure A 2.44 MS (ES^+) of Ind-FO*t*Bu **108**

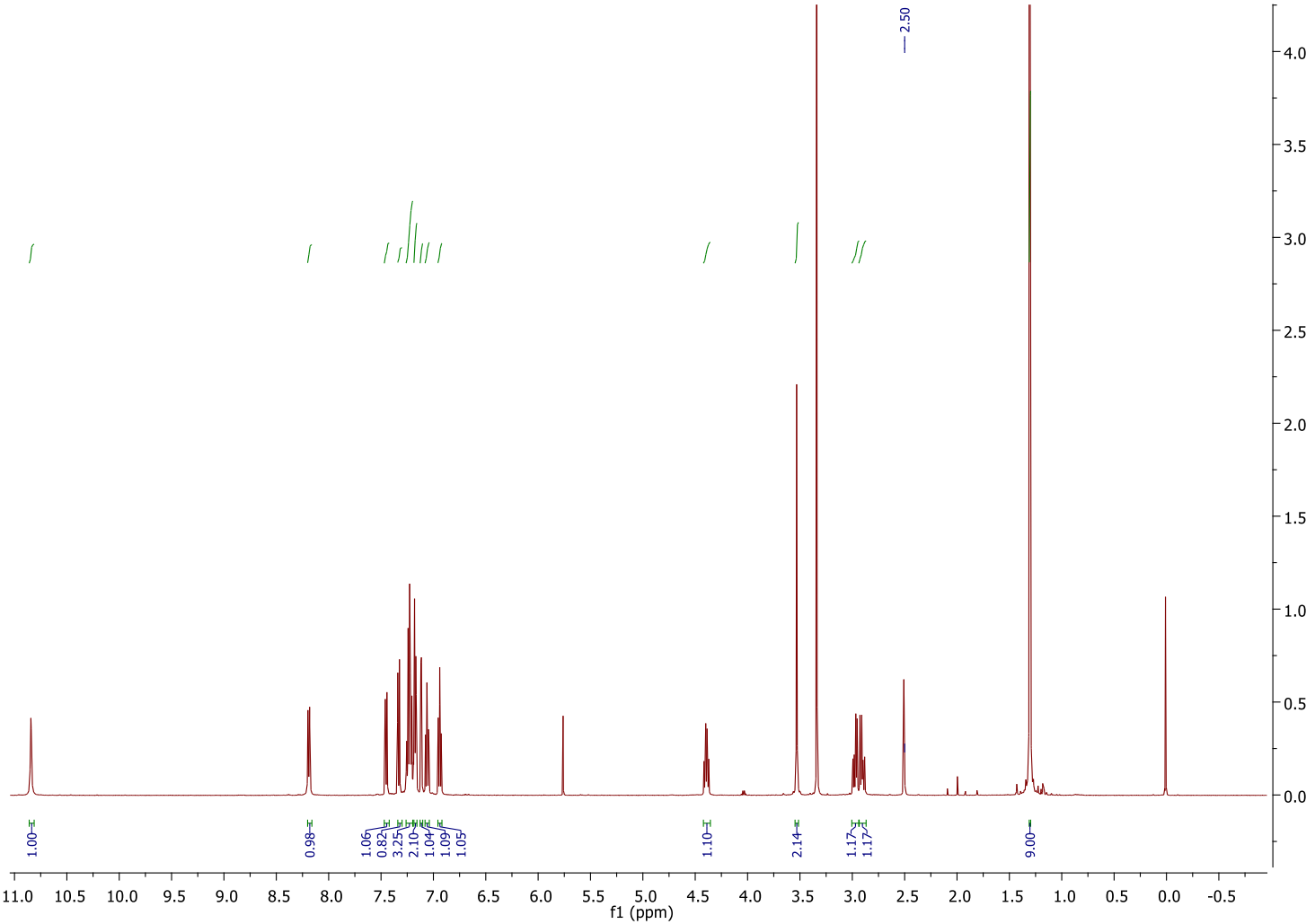

Figure A 2.45 ^{1}H NMR (500 MHz, dmso-d_6) spectrum of Ind-FO*t*Bu **108**

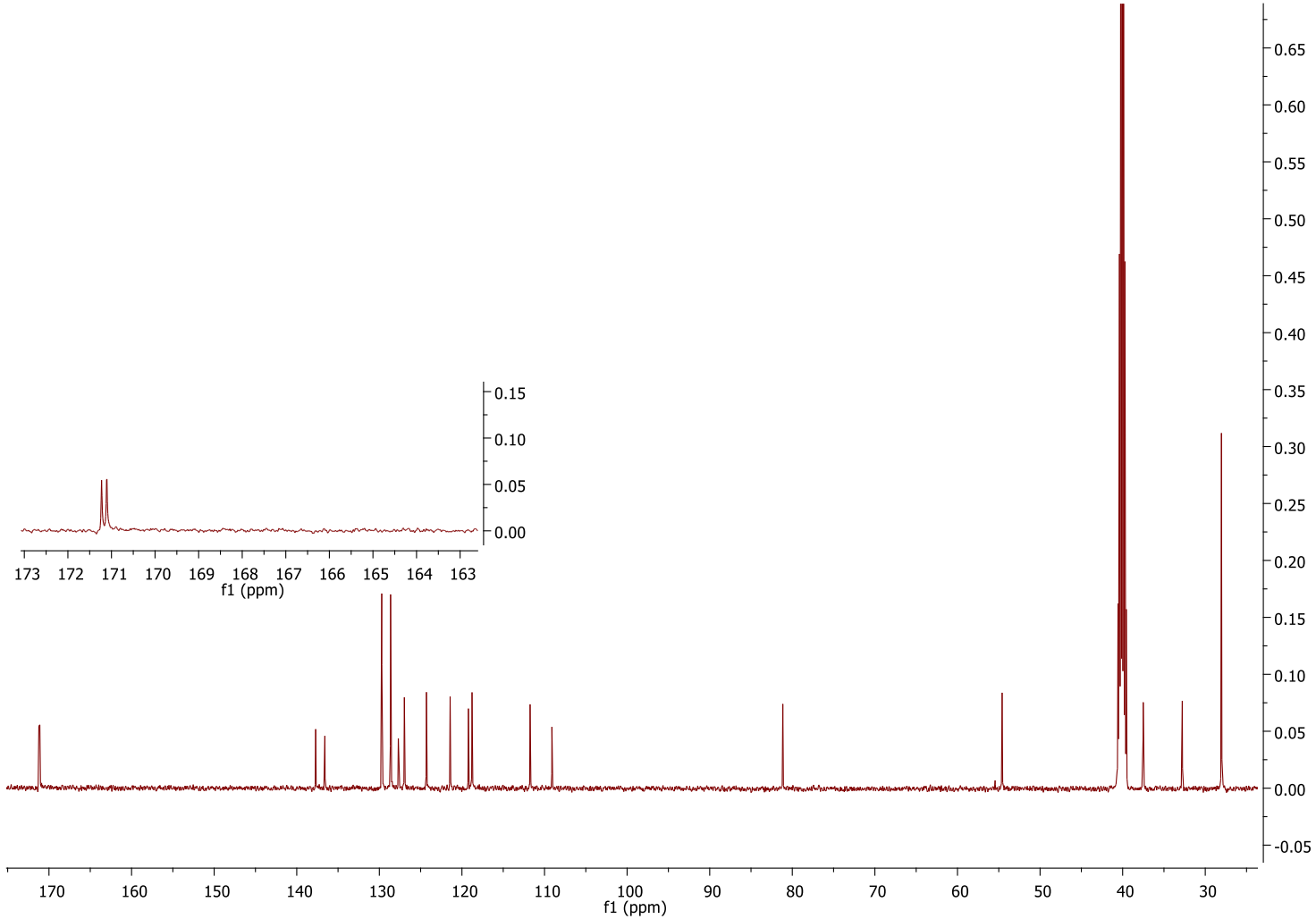

Figure A 2.46 ^{13}C NMR (126 MHz, dmso-d_6) spectrum of Ind-FO*t*Bu **108**

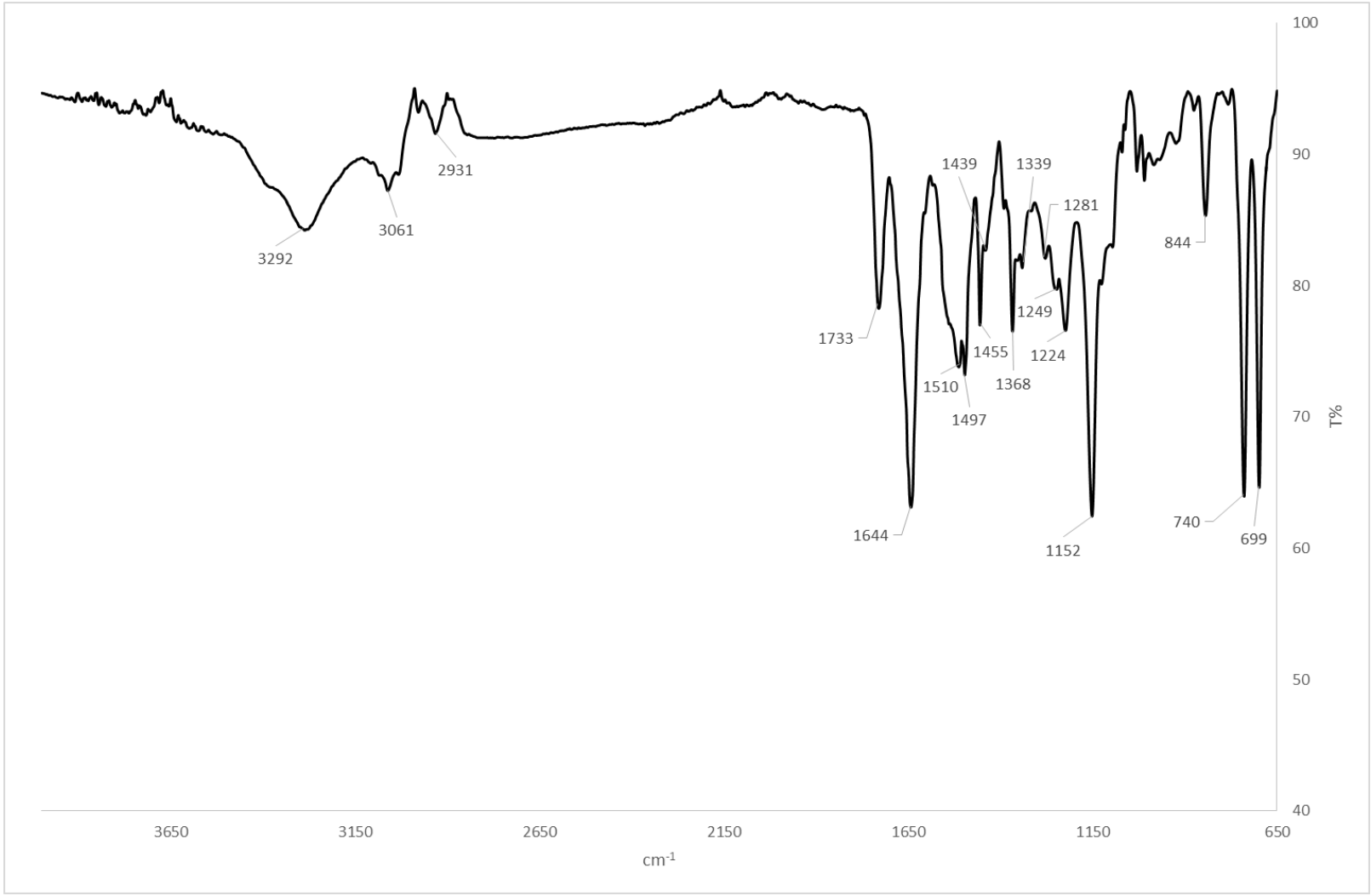

Figure A 2.47 IR spectrum (neat) of Ind-F-FO*t*Bu **110**

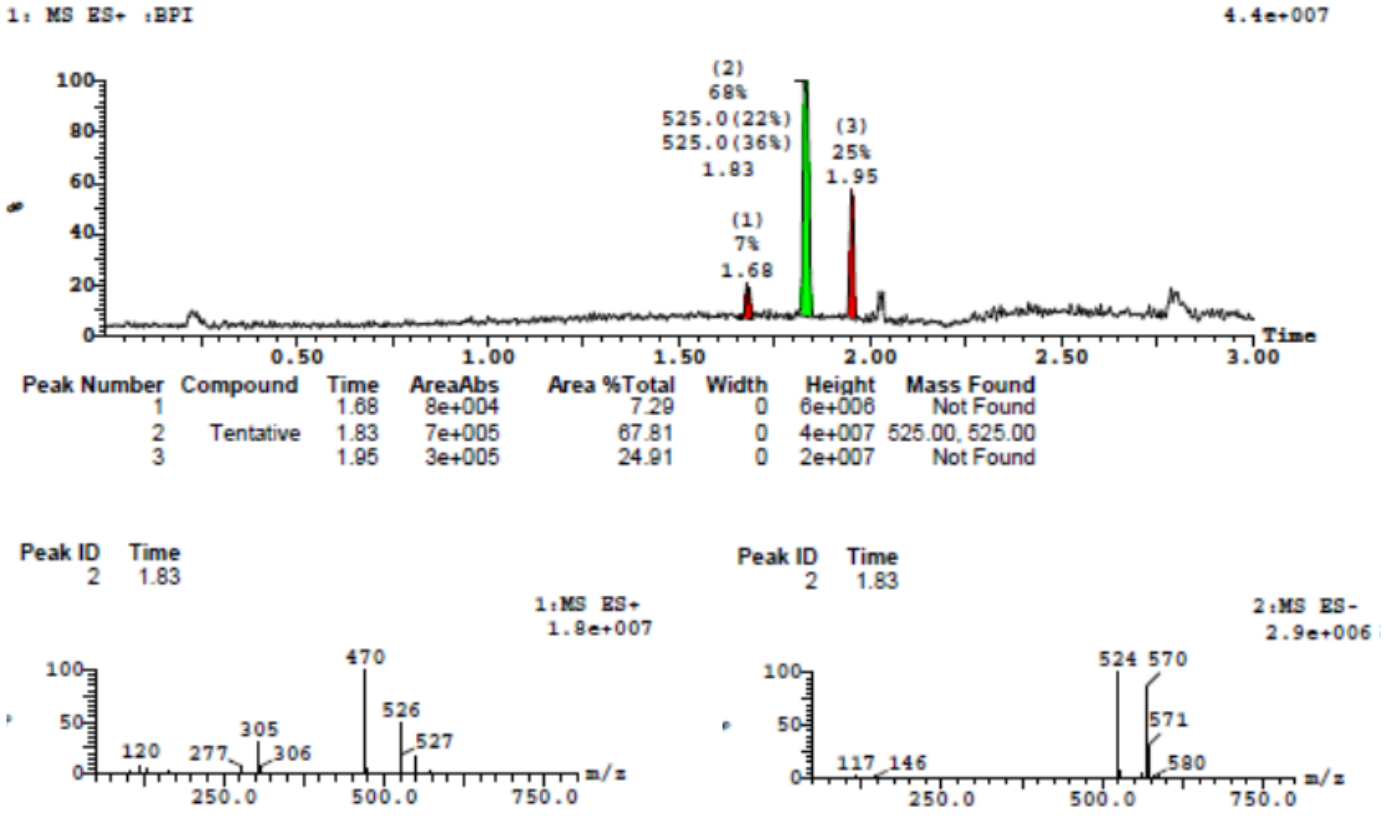

Figure A 2.48 MS (ES^+) and (ES^-) of Ind-F-FO*t*Bu **110**

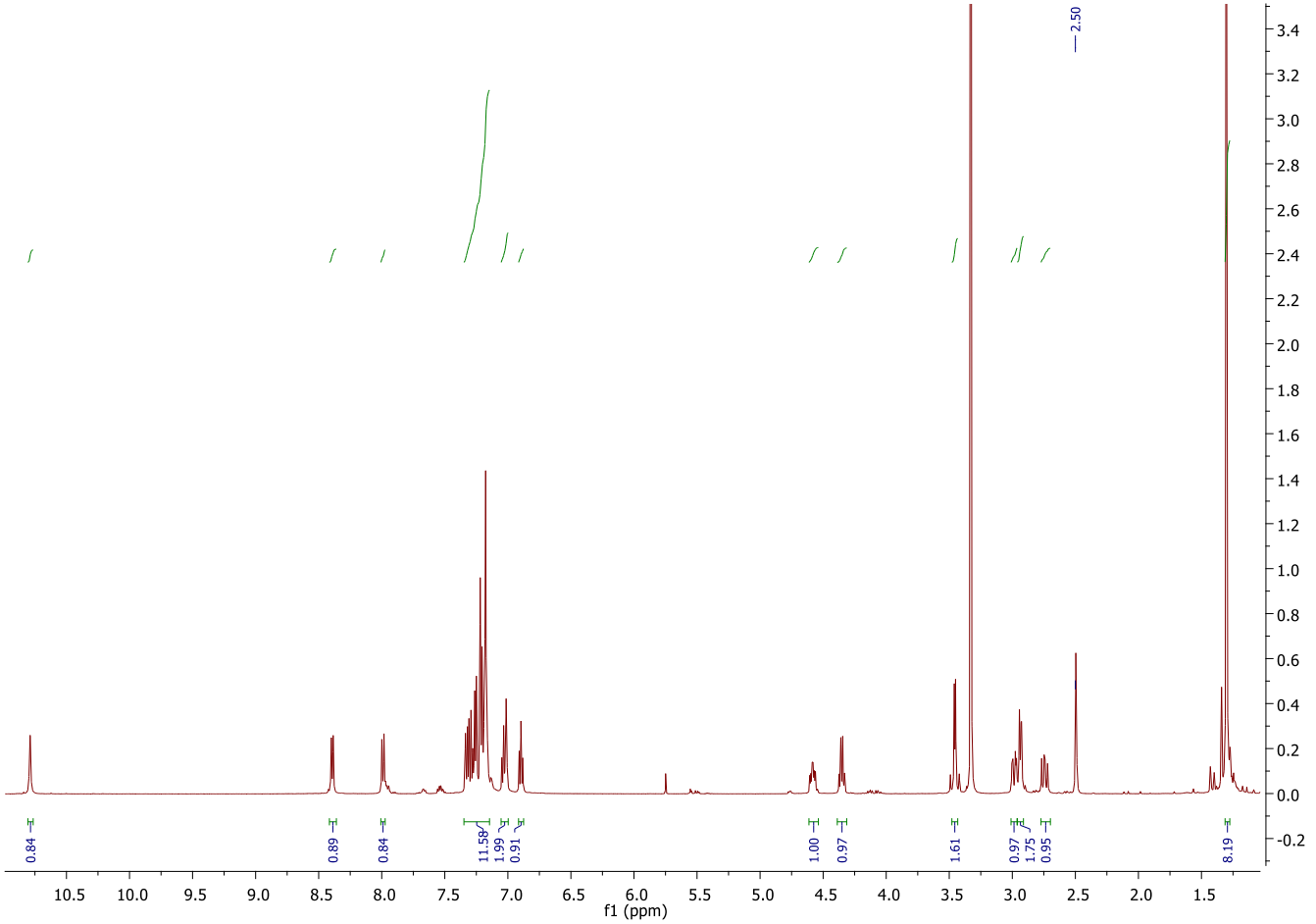

Figure A 2.49 ^{1}H NMR (500 MHz, dmso-d_6) spectrum of Ind-F-FO*t*Bu **110**

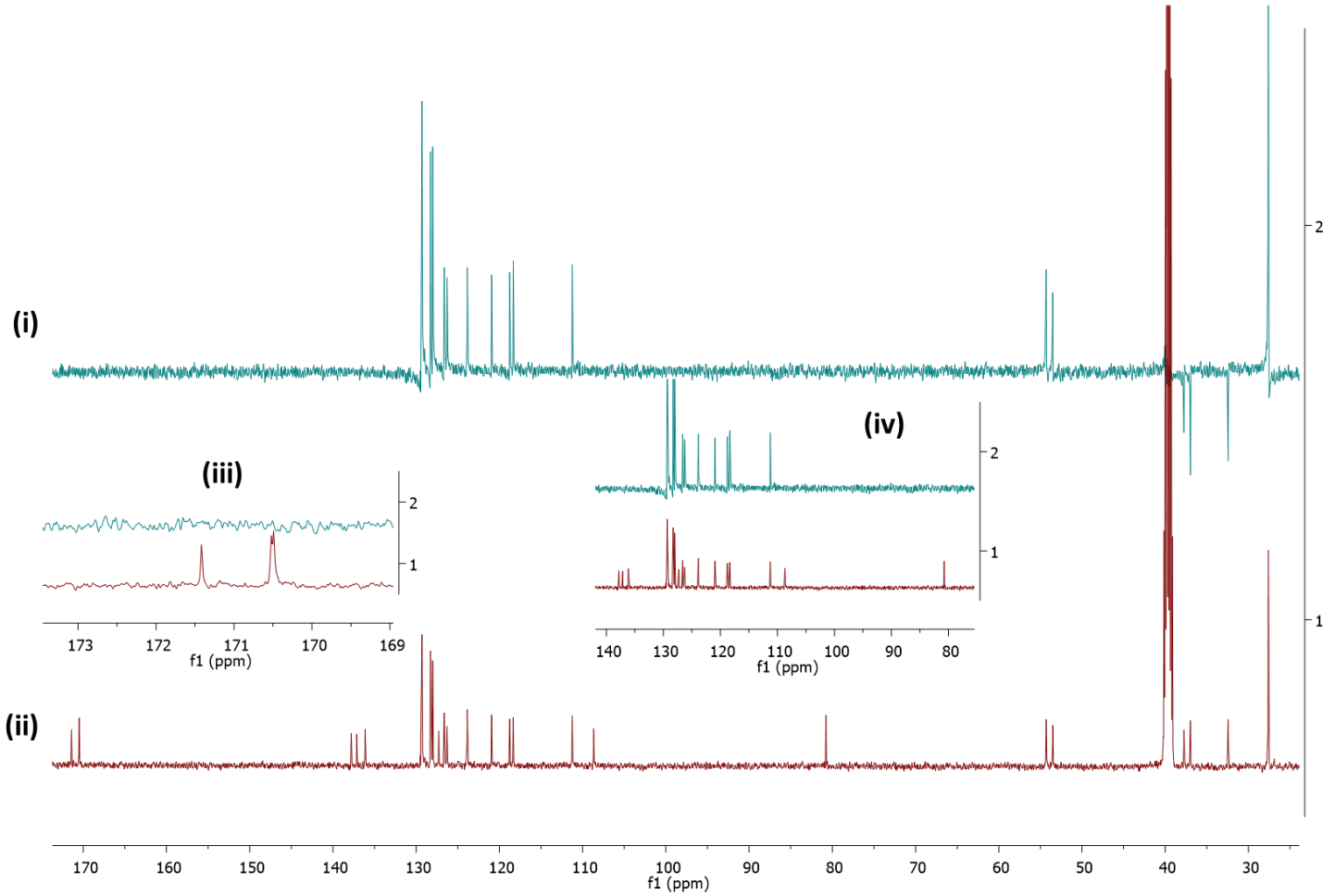

Figure A 2.50 DEPT-135 (i) and ^{13}C NMR (126 MHz, dmso-d_6) (ii) spectrum of Ind-F-FO*t*Bu **110**. Enlarged areas (iii) and (iv)

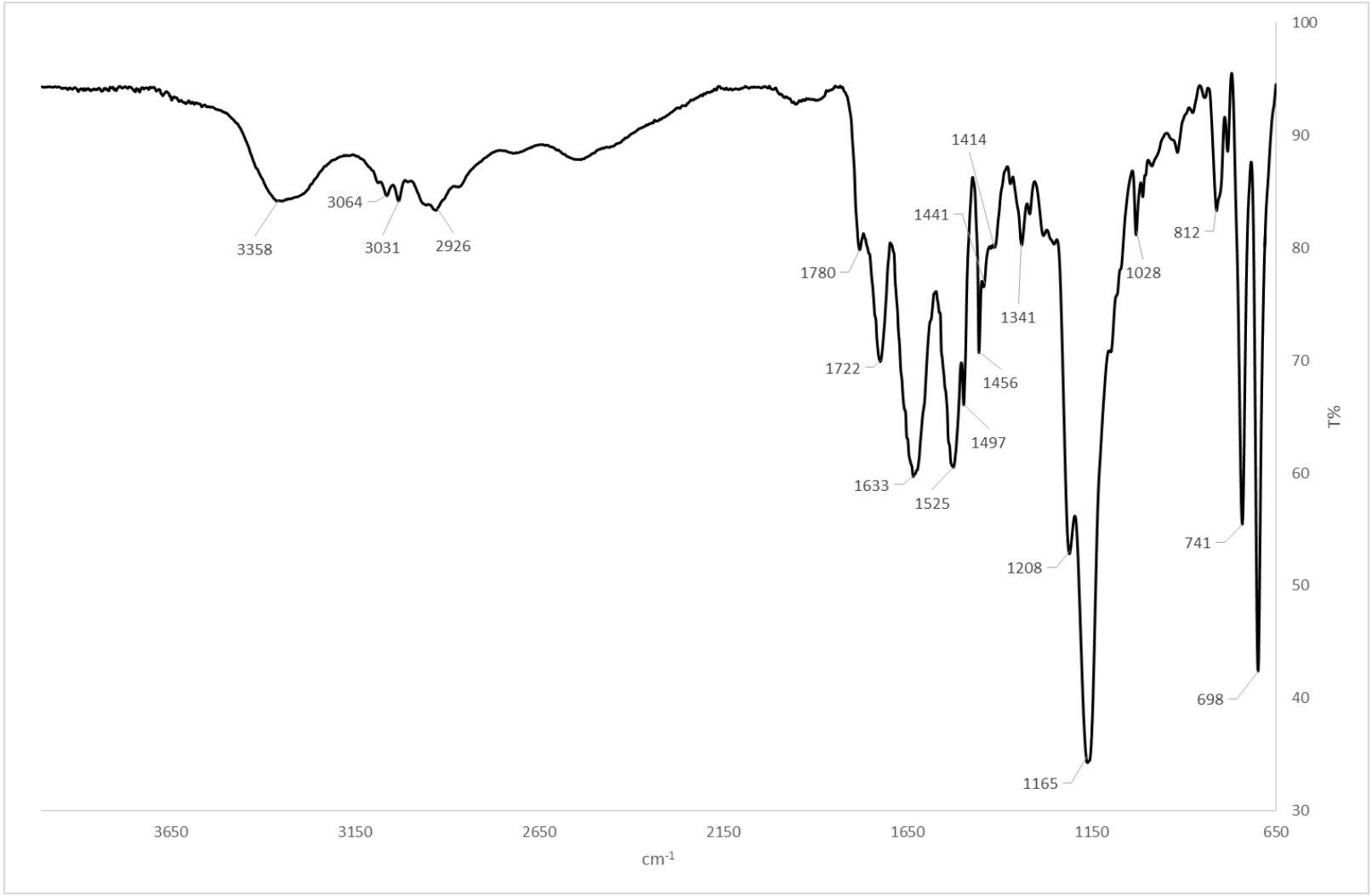

Figure A 2.51 IR spectrum (neat) of Ind-F-F **69**

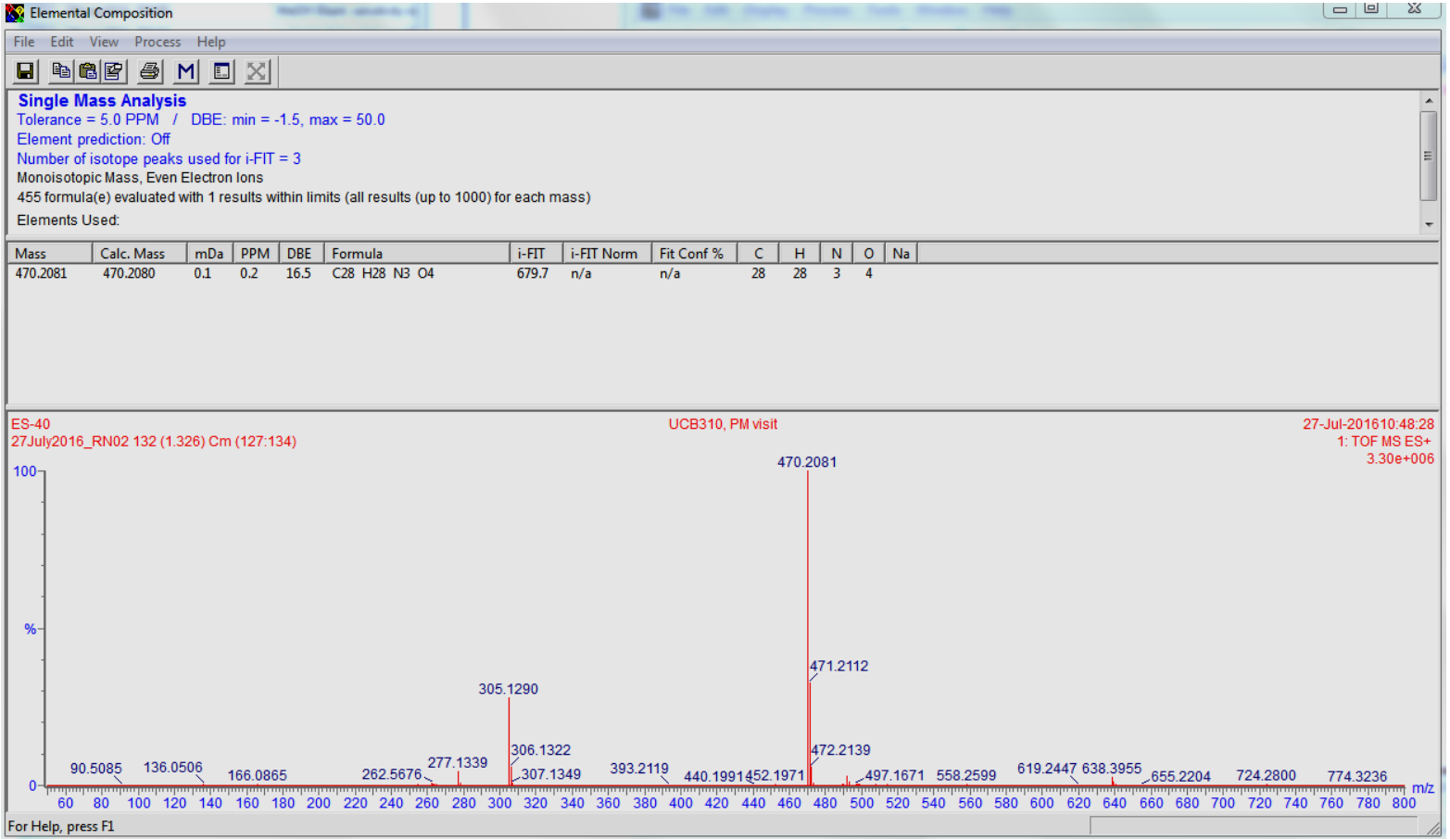

Figure A 2.52 HR-MS of Ind-F-F **69**

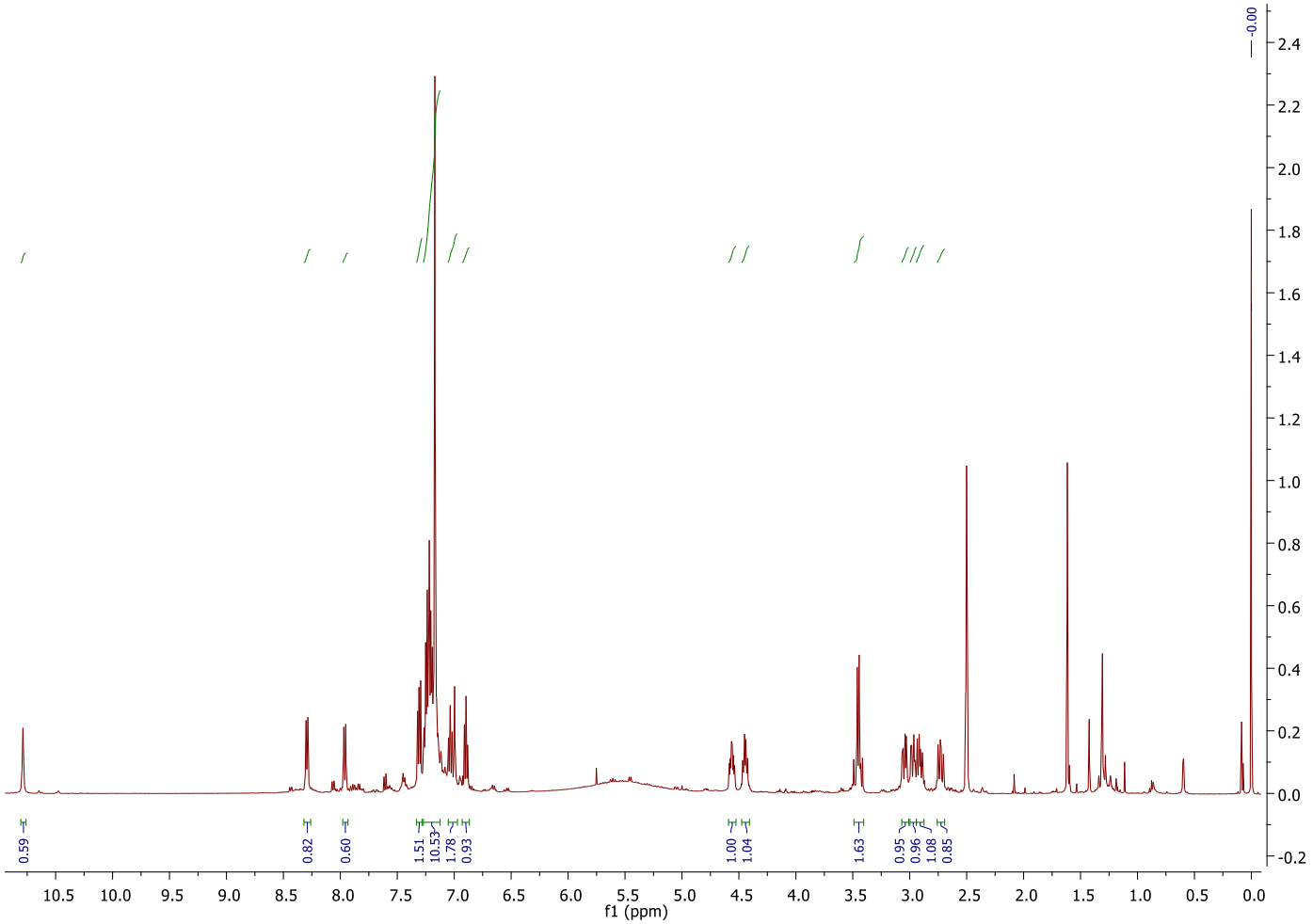

Figure A 2.53 ^{1}H NMR (500 MHz, dmso-d_6) spectrum of Ind-F-F **69**

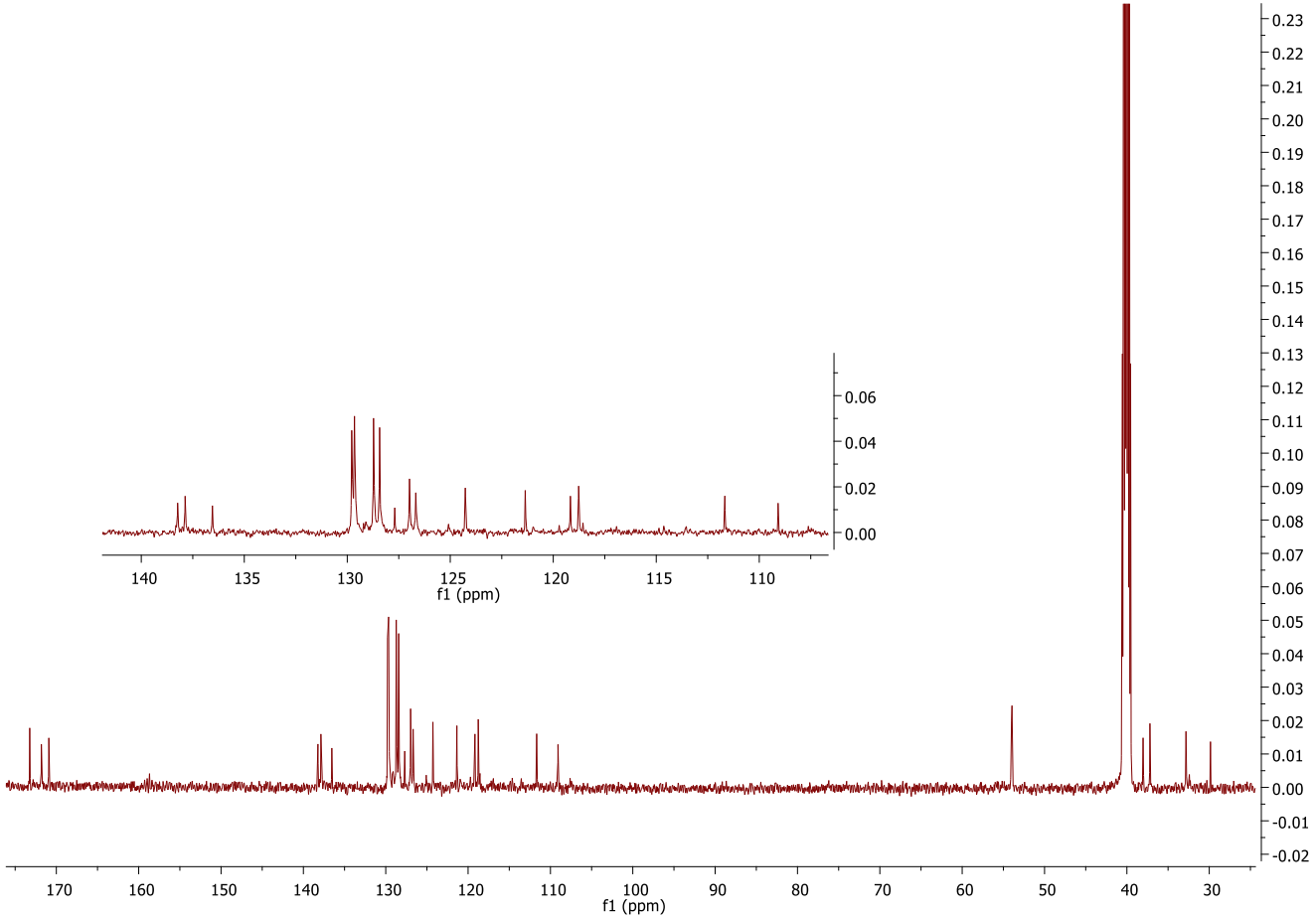

Figure A 2.54 ^{13}C NMR (126 MHz, dmso-d_6) spectrum of Ind-F-F **69**

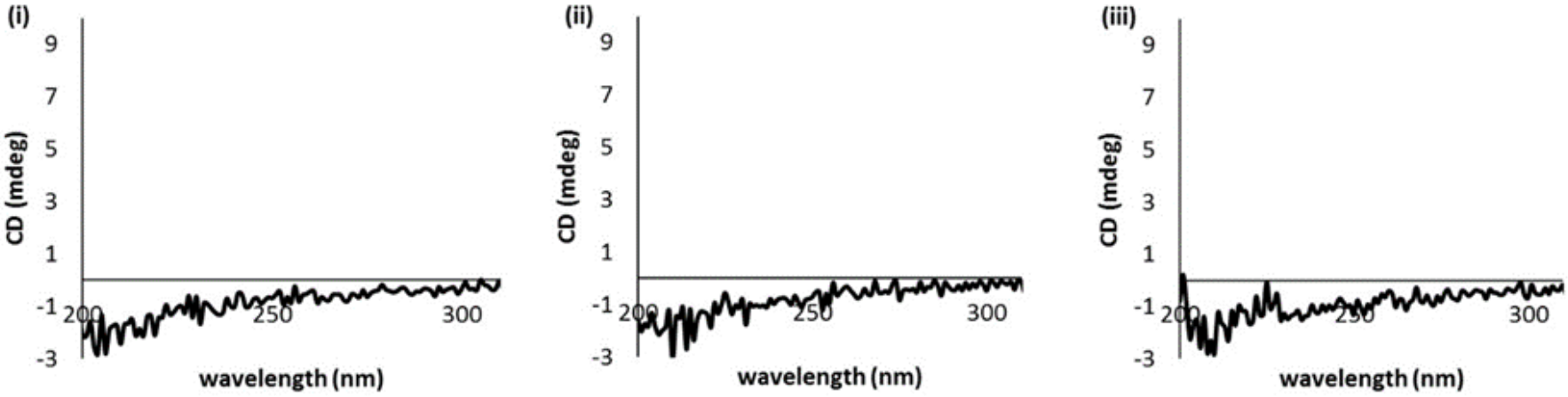

Figure A 4.1 CD spectra of hydrogelators **62**, **63**, **68** in methanol. (i) GalNHFmoc **62**; (ii) GlcNHFmoc **63**; (iii) Fmoc-F-F **68**. All samples were recorded in a cylindrical non-demountable cell of the path length 0.1 mm at a concentration of 0.2 mg/mL.

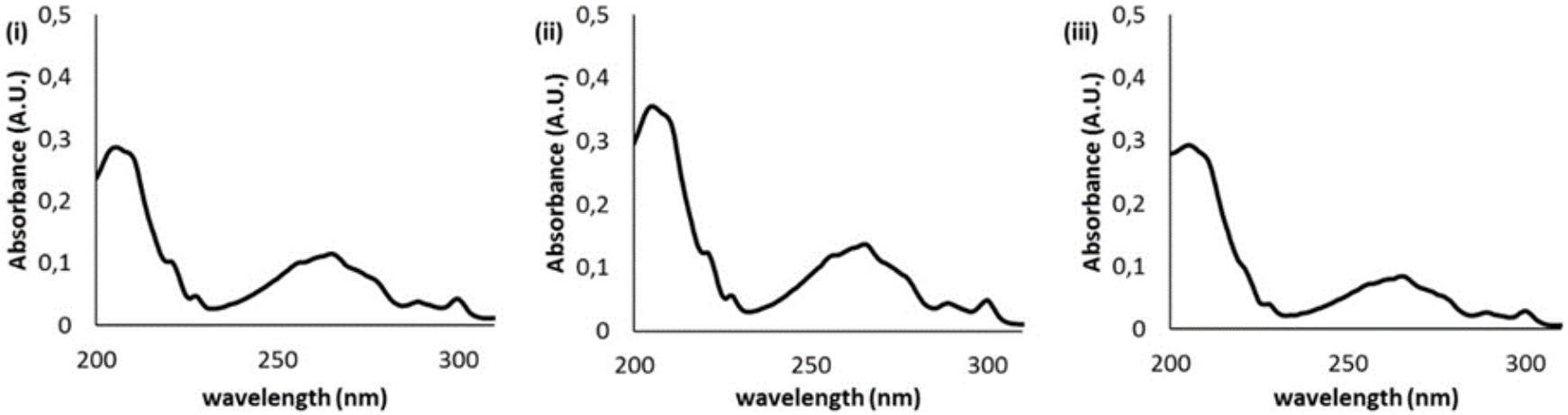

Figure A 4.2 Absorbance spectra of hydrogelators **62**, **63**, **68** in methanol. (i) GalNHFmoc **62**; (ii) GlcNHFmoc **63**; (iii) Fmoc-F-F **68**. All samples were recorded in a cylindrical non-demountable cell of the path length 0.1 mm at a concentration of 0.2 mg/mL.